JOINT DENSITY-FUNCTIONAL THEORY AND ITS APPLICATION TO SYSTEMS IN SOLUTION

A Dissertation

Presented to the Faculty of the Graduate School

of Cornell University

in Partial Fulfillment of the Requirements for the Degree of

Doctor of Philosophy

by

Sahak A. Petrosyan

August 2006

JOINT DENSITY-FUNCTIONAL THEORY AND ITS APPLICATION TO SYSTEMS IN SOLUTION

Sahak A. Petrosyan, Ph.D.

Cornell University 2006

The physics of solvation, the interaction of water with solutes, plays a central role in chemistry and biochemistry, and it is essential for the very existence of life. Despite the central importance of water and the advent of the quantum theory early in the twentieth century, the link between the fundamental laws of physics and the observable properties of water remain poorly understood to this day. The central goal of this thesis is to develop a new formalism and framework to make the study of systems (solutes or surfaces) in contact with liquid water as practical and accurate as standard electronic structure calculations without the need for explicit averaging over large ensembles of configurations of water molecules.

The thesis introduces a new form of density functional theory for the *ab initio* description of electronic systems in contact with a molecular liquid environment. This theory rigorously joins an electron density-functional for the electrons of a solute with a classical density-functional theory for the liquid into a single variational principle for the free energy of the combined system.

Using the new form of density-functional theory for the *ab initio* description of electronic systems in contact with a molecular liquid environment, the thesis then presents the first detailed study of the impact of a solvent on the surface chemistry of Cr_2O_3, the passivating layer of stainless steel alloys. In comparison to a vacuum,

we predict that the presence of water has little impact on the adsorption of chloride ions to the oxygen-terminated surface but has a dramatic effect on the binding of hydrogen to that surface.

The thesis then presents a density-functional theory for water which gives reasonable agreement with molecular dynamics simulation data for the solvation of hard spheres in water and sufficient agreement with experimental data for hydration of inert gas atoms.

By combining the previous ideas, the last study in the thesis presents a model density functional which includes a description of the coupling of the solvent to the electrons of the solute through a pseudopotential without *any* empirical fitting of parameters to solvation data.

BIOGRAPHICAL SKETCH

The author was born on January 23, 1980 in Kislovodsk, Russia. He graduated from high school in 1996 in Yerevan. He obtained Bachelor of Science degree from Moscow Institute of Physics and Technology in 2000 and started his PhD degree at Cornell University. In 2001 he joined Professor Tomas Arias's group where he conducted research in theoretical condensed matter physics until graduation.

To my parents

ACKNOWLEDGEMENTS

I would like to thank Professor Arias for all of his encouragement and inspiration and for teaching me about physics, research and life in general. I want to thank Professor Rigos for our fruitful collaboration and Professor Ashcroft for his insightful comments through the process of writing my thesis.

I would like to thank my lab mates Ivan Daykov for the interesting conversations, Daniel Freedman for his debates about Microsoft, David Roundy for his compelling views, Hande Ustunel, Jean-Francois Briere and Johannes Lischner for making life at the office anything but boring. I would also like to thank my fellow FBI members Saswat Sarangi, Saikat Gosh, Kirill Bolotin, Faisal Ahmad, Umberto Pesavento and Scott Bunch for all of our memorable times. Scott was my roommate for five years and is an unforgettable and irreplaceable friend.

I want to thank Ithaca's Armenian community. Eduard Antonyan, Yeranuhi and Valeri Hakobyan, Khajak Berberian, Lucy and Hrair Missirian, Alice and Sam Sarkissian, Yervant Terzian, and especially Ashot Papoyan, Helen Bisharyan, Gagik and Zara Parsamian, and Karen Mkhoyan who have created a New Armenia in Ithaca.

I would like to thank my father and mother, Aram and Sonya, who have given me their unconditional love, support, and guidance all of my life. I also want to thank my brother Hayk and my sister Genya for their encouragement and friendship. I want to thank Victor, Varsenik and Levon Arvanian for supporting me and making me a part of their family.

Finally, I want to thank my wife Tamara for her great love, support, care and friendship. Her smiles always brighten my days.

TABLE OF CONTENTS

1 Introduction **1**
1.1 Electron density-functional theory 6
1.2 Classical density functional theory of liquids 12
Bibliography 16

Bibliography **16**

2 Joint Density-Functional Theory **19**
Bibliography 25

Bibliography **25**

3 Joint Density-Functional Theory: *Ab Initio* Study of Cr_2O_3 Surface Chemistry in Solution **26**
3.1 Introduction 27
3.2 Theoretical approach: joint density-functional theory 28
3.3 Computational details 29
3.4 Local dielectric theory 30
3.5 Results and discussion 34
3.5.1 Pristine surface 34
3.5.2 Interaction with hydrogen 42
3.5.3 Interaction with chlorine 49
3.5.4 Conclusions 52
Bibliography 58

Bibliography **58**

4 Classical Density-Functional Theory for Water **60**
4.1 Introduction 60
4.2 Failure of traditional weighted-density functional form 62
4.3 Construction of classical density-functional theory for water 68
4.4 Application to hydration of hard spheres 72
4.5 Application to hydration of inert gas atoms 72
4.6 Conclusions and future directions 77
Bibliography 79

Bibliography **79**

5 Joint Density-Functional Theory for Electronic Structure of Solvated Systems **81**
5.1 Introduction 81
5.2 Joint density-functional theory 83

5.3 Construction of approximate functionals 84
5.4 Results and conclusions 91
Bibliography 95

Bibliography **95**

LIST OF TABLES

4.1 Fitted values of parameters in Eq. (4.2) 64
4.2 Properties of uniform bulk water at Standard Ambient Temperature and Pressure (SATP: T=25 °C, P=100.00 kPa) 71
4.3 Solvation energies of inert gas atoms 77

5.1 Fit parameters from (5.2) with comparisons between model and experimental results (at standard conditions of 20°C and atmospheric pressure. (*) The value for $d\gamma/dR$ is theoretical[16]. (See text.) . . 86

LIST OF FIGURES

1.1 A schematic view of the minimization procedure and the breakdown of the final free energy functional A. N_i is the solvent nuclear density, n is the system electron density, V is the electrostatic field created by solute nuclei. 3

3.1 Comparison of the predictions of a simple joint density-functional theory (vertical axis) with established quantum chemical values (horizontal axis) for the electrostatic contribution to the solvation energy of acetamide, acetic acid, methanol, ethanol and methane (from left to right) from Marten *et al.*[21]. 33

3.2 Relaxed structure of a pristine surface slab, side view ([0001] direction runs vertically up the page): oxygen (light gray spheres), chromium (dark gray spheres). The labeling of atomic layers follows Cline *et al.*[11]. 34

3.3 Near-gap energy levels for (a) pristine, (b) hydrogenated, and (c) chlorinated system in (1) vacuum and (2) dielectric: filled levels (solid circles), empty levels (open circles), and partially filled levels (crosses). 36

3.4 Total density of states per electron of pristine supercell slab in vacuum (solid curve) and in solution (virtually indistinguishable dashed curve): occupied states (curve on left), unoccupied states (curve on right), and LSDA atomic eigenvalues (vertical arrows) labeled according to alignment (↑) or anti-alignment (↓) with direction of net atomic spin. 37

3.5 Contour level ($0.68\ e^-/\text{Å}^3$) of the sum of probability densities from the highest energy shoulder of the oxygen $2p$ band, side view ([0001] direction runs vertically up the page): up spin (black surface), and down spin (white surface). Locations of atomic layers are indicated as in Figure 3.2. 39

3.6 Contour level ($0.68\ e^-/\text{Å}^3$) of sum of probability densities from the chromium $sd\uparrow$ band, side view ([0001] direction runs vertically up the page): up spin (black surface), and down spin (white surface). Atomic layers indicated as in Figure 3.2. 40

3.7 Contour level ($0.68\ e^-/\text{Å}^3$) of sum of probability densities from the lowest energy shoulder of the chromium $sd\downarrow$ spin band, side view ([0001] direction runs vertically up the page): up spin (black surface), down spin (white surface). Atomic layers indicated as in Figure 3.2. 41

3.8 Relaxed structure of surface slab with adsorbed hydrogen in (a) vacuum and (b) dielectric: oxygen (light gray spheres), chromium (dark gray spheres), and hydrogen (black spheres). Same view as Figure 3.2 but showing atoms from a single supercell. 43

3.9 Relaxed structure of a single supercell with adsorbed hydrogen in vacuum, top view ([0001] direction normal to page): oxygen (light gray spheres), chromium (dark gray spheres), and hydrogen (black sphere). 44
3.10 Contour level (0.68 $e^-/\text{Å}^3$) of total electron density for hydrogen atom adsorbed on oxygen-terminated (0001) surface in (a) vacuum and (b) dielectric, side view ([0001] direction runs vertically up the page). Atomic layers indicated as in Figure 3.2. Note that most contours are near spherical and appear as balls centered on atoms. 45
3.11 Local density of states within 0.69 Å of the proton for hydrogen interacting with oxygen-terminated (0001) surface in vacuum (solid curve) and solution (dashed curve). Same conventions as Figure 3.4. 46
3.12 Contour level (0.68 $e^-/\text{Å}^3$) of the sum of probability densities associated with oxygen $2p$ surface band in (a) vacuum and (b) dielectric: up spin (black surface), down spin (white surface). Atomic layers indicated as in Figure 3.2. 47
3.13 Contour level (0.68 $e^-/\text{Å}^3$) of the HOMO of hydrogen interacting with the oxygen-terminated (0001) surface in (a) vacuum and (b) dielectric, side view ([0001] direction runs vertically up the page): up spin (black surface), down spin (white surface). Atomic layers indicated as in Figure 3.2. 48
3.14 Relaxed structure of surface interacting with chlorine in vacuum: oxygen (light gray spheres), chromium (dark gray spheres), and chlorine (black sphere): top view ([0001] direction perpendicular to page). 50
3.15 Contour level (0.68 $e^-/\text{Å}^3$) of total electron density for chlorine atom adsorbed on oxygen-terminated (0001) surface in (a) vacuum and (b) dielectric, side view ([0001] direction runs vertically up the page). Atomic layers indicated as in Figure 3.2. Note that densities are such that the contours appear spherical. 51
3.16 Local density of states within 1.6 Å of the chlorine nucleus for chlorine interacting with the oxygen-terminated (0001) surface in vacuum (solid curve) and solution (dashed curve). Same conventions as Figure 3.4. 53
3.17 Contour level (0.68 $e^-/\text{Å}^3$) of HOMOs and LUMOs (equivalent in this case) of chlorine interaction with oxygen-terminated (0001) surface in (a) vacuum and (b) dielectric, side view ([0001] directions runs vertically up the page). Atomic layers indicated as in Figure 3.2. 54

4.1 Oxygen-oxygen total correlation function in liquid water: experimentally determined data of [19] (squares), Fourier transform of fitted analytic function Eq. (4.2) (curve) 64
4.2 Direct oxygen-oxygen correlation function for liquid water in Fourier space extracted from experimental data 65

4.3 Two roots of Eq. (4.1) for $w(k)$ (real part) 66
4.4 Direct correlation function $k_BTc(k)$ from Figure 4.2 and the residual $\chi(k)$. 70
4.5 Free energy density of water as a function of its density at SATP . 71
4.6 Surface tension of a hard sphere of radius R in water at SATP. Solid line denotes the results of our classical density-functional theory calculations. Molecular simulation results for a cavity in SPC/E water are indicated by diamonds [23]. Dashed line corresponds to macroscopic surface tension of water. R is defined as the distance of closest approach between molecular centers and sphere center. . 73
4.7 Interaction of Argon and a water molecule. Each diamond corresponds to a specific orientation. Also presented are the Boltzmann average potential (solid line) and the minimum potential (dot-dashed line). 75

5.1 Comparison of energy of interaction of water molecule with an atom of neon as a function of neon-oxygen distance: results from orientation independent pseudopotential (solid curve), orientally averaged *ab initio* data (centers of error bars), typical (1σ) range of values as a function of orientation (range of error bars). 88
5.2 Short-ranged repulsive potential added to prevent collapse of liquid density $N(r)$ into the strong electric fields within the atomic cores. Once prevention of this artificial collapse is achieved, the final results are insensitive to the choice of this potential. 90
5.3 Spherical average of $N(r)$ about the oxygen nucleus of an explicit water molecule in solution scaled to the bulk liquid density, corresponding to the correlation function $g_{OO}(r)$ measured in experiments on liquid water. 92
5.4 Computed (vertical axis) versus experimental (horizontal axis) solvation energies for water, ethanol, methanol and methane (from left to right): perfect agreement (diagonal line), published quantum chemistry values ([20] for all but water, [21] for water) with dielectric contribution only (open squares) and including cavitation terms (closed squares), preliminary results from joint density functional theory (open circles). 93

Chapter 1

Introduction

The physics of solvation, the interaction of water with solutes, plays a central role in chemistry and biochemistry, and is essential for the very existence of life. As early as the fourth century BC, water was identified by the Greek philosopher Empedocles as one of the four classical elements needed to understand the world *ab initio*, directly from first principles. Despite the central importance of water and the advent of the quantum theory early in the twentieth century, the link between the fundamental laws of physics and the observable properties of water remain poorly understood to this day. The reason for this can be traced to the famous statement of Paul Dirac[1]

> The underlying physical laws necessary for the mathematical theory of a large part of physics and the whole of chemistry are thus completely known, and the difficulty is only that the exact application of these laws leads to equations much to complicated to be soluble. It therefore becomes desirable that approximate practical methods of applying quantum mechanics should be developed, which can lead to an explanation of the main features of complex atomic systems without too much computation.

Fortunately, in large measure, this prediction has proved true, and there has been tremendous progress since 1929 in explaining chemistry from fundamental physics. To Dirac's credit, much of this progress has come not from directly solving the equations which Dirac had in mind, but from formulating new approximate equations from the fundamental laws, particularly in the form of density functional

theory, for which Walter Kohn was awarded the Nobel prize in 1998.

The density-functional approach has been applied successfully to a wide range of problems in physical chemistry ranging from plasticity, diffusion and surface reconstruction to melting and chemical reactions [2]. Despite this progress, *ab initio* understanding of solvation remains out of reach — largely because the liquid state of water can only be understood quantitatively by computing an ensemble of a large number of water molecules in a large number of different configurations. For instance, a recent report [3] of a density-functional calculation with a modest number of 512 molecules required use of the fastest publicly disclosed supercomputing cluster in the world as of June 2006. The central goal of this thesis is to develop a new formalism and framework to make the study of systems (solutes or surfaces) in contact with liquid water as practical and accurate as standard electronic structure calculations without the need for explicit averaging over large ensembles of configurations of large numbers of water molecules.

The remainder of this introduction reviews the basic theories used in the thesis, Hohenberg-Kohn-Sham density functional theory for electronic systems (Section 1.1) and the so-called "classical" density-functional theory of liquids (Section 1.2). In this thesis, we write "classical" in quotation marks because the classical density-functional theory of liquids applies to classical as well as quantum liquids and has been applied successfully, for example, to liquid helium [4]. This distinction is important because the zero point motion of the protons in water is thought to be an important aspect of the underlying physics of the liquid [5].

Chapter 2 introduces a new form of density-functional theory for the *ab initio* description of electronic systems in contact with a molecular liquid environment. This theory *rigorously* joins an electron density-functional for the electrons of a

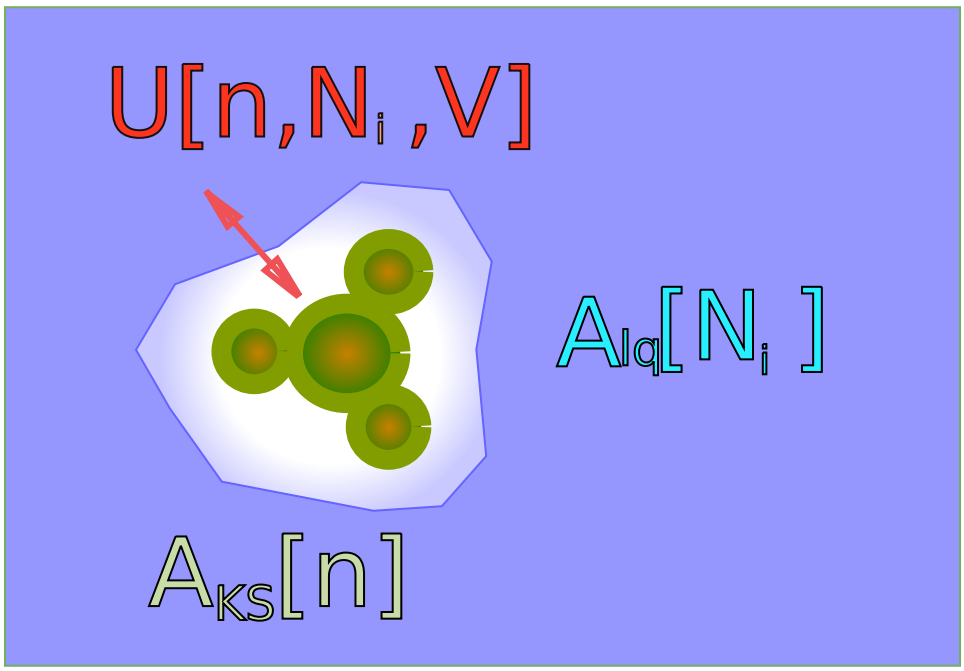

Figure 1.1: A schematic view of the minimization procedure and the breakdown of the final free energy functional A. N_i is the solvent nuclear density, n is the system electron density, V is the electrostatic field created by solute nuclei.

solute with a classical density-functional theory for the liquid into a single variational principle for the free energy of the combined system. The theorem that we prove shows that the thermodynamics of a system and its electrons (the *solute*) in equilibrium with a liquid environment (the *solvent*) can be described rigorously in terms of a *joint density-functional theory* (JDFT) between the electrons in the system and the molecules comprising the solvent. The physics of the equilibrium between the solute and solvent (cavity formation, dielectric screening, dispersion, and repulsion) are then all determined in a single variational principle. While this new theory is rigorous and exact *in principle*, like electron density-functional theory, it introduces an unknown functional which must be approximated in order for calculations to be performed.

Figure 1.1 shows a sketch of the overall system. The final free energy functional A is written as a sum of three terms A_{KS}, A_{lq} and U. $A_{KS}[n(r)]$ is standard universal Kohn-Sham electron-density functional of the explicit system when in isolation, $A_{lq}[\{N_i(r)\}]$ is the "classical" density functional for the liquid solvent environment when in isolation, and $U[n(r), \{N_i(r)\}, V(r)]$ describes the coupling between the solute and the solvent. In these terms, $n(r)$ represents the electron density associated with the explicit system, $\{N_i(r)\}$ represents the molecular density associated with the solvent environment, and $V(r)$ represents the electrostatic potential from the nuclei of the explicit system. Note that here we do not attempt to separate the Hamiltonian of the combined system into an explicit system Hamiltonian, an environment Hamiltonian, and coupling Hamiltonian. We do not attempt this because, as described in Section 1.1 below, the fundamental indistinguishability of the electrons makes such a separation less than straightforward. While the issue of indistinguishability is less severe in the density-functional level, there remain a few subtleties. For instance, the electron density $n(r)$ "associated with the explicit system" cannot be uniquely defined. Mathematically, this simply means that, while the minimum value of $A_{KS}[n(r)] + A_{lq}[\{N_i(r)\}] + U[n(r), \{N_i(r)\}, V(r)]$ is well defined, many possible $n(r)$ lead to the minimum value. Chapter 2 discusses this point in detail.

Chapter 3 then presents our first, very simple model form for the unknown functional, which we call the *local dielectric approximation*. We show that, even with this very simple model and a single fit parameter, the theory produces results which agree well with the current state-of-the-art in solvation quantum chemistry, dielectric cavity calculations, which employ a large number of fit parameters. Encouraged by the apparent success of the model in giving reliable energies, Chapter 3

then applies the resulting approach to the first detailed study of the impact of a solvent on the surface chemistry of Cr_2O_3, the passivating layer of stainless steel alloys. In comparison to a vacuum, the new model predicts that the presence of water has little impact on the adsorption of chloride ions to the oxygen-terminated surface but has a dramatic effect on the binding of hydrogen to that surface. These results indicate that the dielectric screening properties of water are important to the passivating effects of the oxygen-terminated surface.

Although we find the aforementioned agreement with quantum chemistry dielectric cavity calculations quite encouraging, one should not take the fact that we require only a single fit parameter to imply that the model captures all of the essential underlying physics. Among the weak points of this first, very simple model are that it ignores (a) the effects of forming a cavity in the fluid, (b) the energetics associated with the short-range repulsive interactions which ultimately lead to such cavity formation, (c) the fact that the dielectric response of the environment is in general non-local in space. The subsequent chapters of the thesis represent a first attempt at addressing these weaknesses.

To address cavity effects, Chapter 4 advances the state of the art for functionals of liquid water by itself, a necessary ingredient to address the cavitation effects mentioned above. This chapter introduces a new computationally efficient classical density-functional theory for water, which gives relatively accurate cavitation energies (20% error in the worst case) and attempts to apply it to the challenging problem of the hydration of inert gas atoms. We find encouraging agreement (at the level of 0.1 eV) for the solvation of inert gas atoms in water, but clearly more work is needed. In particular, some way of addressing the orientation of the molecules in a computationally efficient manner is sorely needed.

To address short-range interactions between solute and solvent and to explore the importance of non-local dielectric effects, Chapter 5 presents an approximate density-functional theory which includes, in addition to a description of cavitation effects through a classical density-functional theory, a description of dielectric effects through a model non-local polarizability and a description of the coupling of the solvent to the electrons of the solute through a pseudopotential. Without *any* empirical fitting of parameters to solvation data, this theory predicts solvation energies at least as well as state-of-the-art quantum-chemical cavity approaches, which do employ such fitting. Once again, while we feel that this agreement without fit parameters strongly suggests that joint density-functional theory is a promising avenue to understand the physics of solvation at a *quantitative* level, one should not take the lack of fit parameters to imply that we have captured all of the underlying physics. The resulting approximate functional clearly involves significant modeling of effects, particularly dielectric screening. Chapter 4 then concludes the thesis with some suggestions of directions for future research which would capture much more of the underlying physics.

1.1 Electron density-functional theory

The many-body time-dependent Schrödinger equation (with relativistic corrections) captures the physics of a large number of problems in the electronic structure of matter. In most cases, however, one is concerned with atoms and molecules without time dependent interactions, so we may focus on the time-independent Schrödinger equation. For an isolated N-electron atomic or molecular system in the Born-Oppenheimer non-relativistic approximation, this equation is

$$\hat{H}\Psi = E\Psi, \tag{1.1}$$

where E is the electronic energy, $\Psi = \Psi(\mathbf{x}_1, \mathbf{x}_2, ..., \mathbf{x}_N)$ is the (fully antisymmetric) wave function, and $\hat{H}$ is the Hamiltonian operator,

$$\hat{H} = \sum_{i=1}^{N}(-\frac{1}{2}\nabla_i^2) + \sum_{i=1}^{N} v(\mathbf{r}_i) + \sum_{i<j}^{N} \frac{1}{r_{ij}} + \sum_{\alpha<\beta} \frac{Z_\alpha Z_\beta}{R_{\alpha\beta}} \tag{1.2}$$

in which

$$v(\mathbf{r}_i) = -\sum_{\alpha} \frac{Z_\alpha}{r_{i\alpha}} \tag{1.3}$$

is the external potential acting on electron i, the potential due to nuclei of charges Z_α at distances $r_{i\alpha}$ from the electrons. The coordinates $\mathbf{x}_i$ of electron i comprise space coordinates $\mathbf{r}_i$ and spin coordinates s_i. When additional fields are present, of course, (1.3) contains extra terms.

We may write (1.2) more compactly as

$$\hat{H} = \hat{T} + \hat{V}_{ne} + \hat{V}_{ee} + \hat{V}_{nn} \tag{1.4}$$

where

$$\hat{T} = \sum_{i=1}^{N}(-\frac{1}{2}\nabla_i^2) \tag{1.5}$$

is the kinetic energy operator,

$$\hat{V}_{ne} = \sum_{i=1}^{N} v(\mathbf{r}_i) \tag{1.6}$$

is the electron-nucleus attraction energy operator,

$$\hat{V}_{ee} = \sum_{i<j}^{N} \frac{1}{r_{ij}} \tag{1.7}$$

is the electron-electron repulsion energy operator, and

$$\hat{V}_{nn} = \sum_{\alpha<\beta} \frac{Z_\alpha Z_\beta}{R_{\alpha\beta}} \tag{1.8}$$

is the the nucleus-nucleus repulsion energy. In the Born-Oppenheimer approximation it is immaterial whether one solves (1.1) for E without V_{nn} term and adds

V_{nn} afterward, or includes V_{nn} in the definition of $\hat{H}$. In the treatment of infinite solids or liquids, however, it is important to keep in mind that thermodynamic limit exists only for charge neutral systems [6].

In the context of an explicit system in contact with an environment, one could imagine separating the total Hamiltonian into a system part $H_{sys} = T+V_{nn}+V_{ne}+V_{ee}$, an environment part $H_{env} = T' + V_{n'n'} + V_{n'e'} + V_{e'e'}$, and an interaction part $H_{int} = V_{nn'}+V_{ne'}+V_{n'e}+V_{ee'}$, where the terms are written just as above, but with T, n, e referring to the electron kinetic energy, the nuclei and electrons of the explicit system and T', n' and e' referring to the respective quantities of the environment. However, separating terms directly like this is not sensible because the electrons are indistinguishable. One would be tempted to write $T' = -\frac{1}{2}\sum_{i'} \nabla^2_{i'}$, where i' ranges over only the electrons of the environment, but indistinguishability forbids such a distinction. To see that such an operator does not belong properly to the Hilbert space of fully antisymmetric wave functions, we note that, without some additional assumptions, there is no way to write an expression for T' in second quantized notation. On the other hand, it is always mathematically possible to write the total electron density as a sum of two densities, each integrating to the number of electrons we ascribe to the system and the environment, respectively. The latter is the approach we take in Chapter 2, where we discuss in depth the subtleties associated with such apportionment of the electron densities.

When a system is in the state Ψ, which may or may not satisfy (1.1), the average of many measurements of the energy is given by the formula

$$E[\Psi] = \frac{<\Psi|\hat{H}|\Psi>}{<\Psi|\Psi>} \tag{1.9}$$

where

$$<\Psi|\hat{H}|\Psi> = \int \Psi^* \hat{H} \Psi d\mathbf{x} \tag{1.10}$$

Since, furthermore, each particular measurement of the energy gives one of the eigenvalues of $\hat{H}$, we immediately have

$$E[\Psi] \geq E_0 \tag{1.11}$$

The energy computed from a guessed Ψ is an upper bound to the true ground-state energy E_0. Full minimization of the functional $E[\Psi]$ with respect to all allowed N-electron wave functions will give the true ground state Ψ_0 and energy $E[\Psi_0] = E_0$; that is,

$$E_0 = \min_{\Psi} E[\Psi] \tag{1.12}$$

Eq. (1.9) tells us that the ground state energy can be found by minimizing $< \Psi|\hat{H}|\Psi >$ over all normalized, antisymmetric N-particle wave functions,

$$E = \min_{\Psi} < \Psi|\hat{H}|\Psi > . \tag{1.13}$$

Following Levy [7], we now separate the minimization of Eq. (1.13) into two steps. First we consider all wave functions Ψ which yield a given density $n(\mathbf{r})$, and minimize over those wave functions,

$$\min_{\Psi \to n} < \Psi|\hat{H}|\Psi >= \min_{\Psi \to n} < \Psi|\hat{T} + \hat{V}_{ee}|\Psi > + \int d^3r v(\mathbf{r})n(\mathbf{r}), \tag{1.14}$$

where we have exploited the fact that all wave functions that yield the same $n(\mathbf{r})$ also yield the same $< \Psi|\hat{V}_{ne}|\Psi >$. Then we define the universal functional,

$$F[n] = \min_{\Psi \to n} < \Psi|\hat{T} + \hat{V}_{ee}|\Psi > . \tag{1.15}$$

Finally we minimize over all N-electron densities $n(\mathbf{r})$,

$$E = \min_{n} E_v[n] = \min_{n} \left\{ F[n] + \int d^3\mathbf{r} v(\mathbf{r})n(\mathbf{r}) \right\}, \tag{1.16}$$

where of course $v(\mathbf{r})$ is held fixed during the minimization. The minimizing density is then the ground state density. Equation (1.16) is known as Hohenberg-Kohn [8] theorem and is at the foundation of density-functional theory.

In order for the functional $F[n]$ to be defined via Eq. (1.15) for some density $n(\mathbf{r})$, there must be at least one wave function Ψ which yields that density $n(\mathbf{r})$. This means that the functional $F[n]$ is defined for any density $n(\mathbf{r})$ which can be obtained from some antisymmetric wave function. Density functions satisfying this condition are called N-representable. It can be proved [9] that a density $n(\mathbf{r})$ is N-representable if $n(\mathbf{r}) \geq 0$ and $\int n(\mathbf{r})d\mathbf{r} = N$.

For a system of non-interacting electrons $\hat{V}_{ee}$ of Eq. (1.7) vanishes, so $F[n]$ of Eq. (1.15) reduces to

$$T_s[n] = \min_{\Psi \to n} < \Psi|\hat{T}|\Psi > = < \Phi^{min}|\hat{T}|\Phi^{min} > \tag{1.17}$$

where the minimizing wave function Φ^{min} for a given density will be a single Slater determinant or a linear combination of some N orbitals $\phi_i(r)$. Now we approximate the electron-electron interaction $\hat{V}_{ee}$ term as

$$U[n] = \iint \frac{1}{2} \frac{n(r)n(r')}{|r - r'|}$$

and define exchange-correlation energy functional $F_{xc}[n]$ by

$$F[n] = T_s[n] + U[n] + F_{xc}[n]$$

The Lagrange multiplier equations corresponding to the minimization in Eq. (1.16) can now be written as

$$\left\{ -\frac{1}{2}\nabla^2 + v(\vec{r}) + \int \frac{n(\vec{r})}{|\vec{r} - \vec{r}'|} dr' + \frac{\delta F_{xc}[n]}{\delta n(\vec{r})} \right\} \phi_i(r) = \epsilon_i \phi_i(r). \tag{1.18}$$

Equations (1.18) are called Kohn-Sham [10] equations and $\phi_i(r)$ are called Kohn-Sham orbitals.

$F_{xc}[n]$ is not known exactly and has to be approximated in practice. Development of approximate exchange-correlation functionals is an active area of research today [11, 12]. The simplest approximation is the local density approximation (LDA) [10], where $F_{xc}[n(r)]$ is approximated as

$$F_{xc}^{LDA}[n(r)] = \int f_{xc}(n(\vec{r}))d\vec{r}$$

where $f_{xc}(n)$ is the exchange-correlation energy density of a uniform electron gas of density n. For spin polarized systems local spin density approximation (LSDA) [13] is very popular in solid state physics

$$F_{xc}^{LSDA}[n_\uparrow, n_\downarrow] = \int f_{xc}(n_\uparrow(\vec{r}), n_\downarrow(\vec{r}))d\vec{r}$$

where $f_{xc}(n_\uparrow, n_\downarrow)$ is the known [14] exchange-correlation energy density for an electron gas of uniform spin densities ($n_\uparrow$, $n_\downarrow$). In this thesis we use the local spin density approximation for the electron density-functional exchange-correlation term.

More recently generalized gradient approximations (GGA's) [11, 12] have become popular in quantum chemistry,

$$F_{xc}^{GGA}[n_\uparrow, n_\downarrow] = \int f_{xc}(n_\uparrow, n_\downarrow, \nabla n_\uparrow, \nabla n_\downarrow)d\vec{r}$$

$f_{xc}(n_\uparrow, n_\downarrow)$ in LSDA is uniquely defined in a sense that a uniform electron gas with $n_\uparrow$, $n_\downarrow$ exists. In that sense, $f_{ex}(n_\uparrow, n_\downarrow, \nabla n_\uparrow, \nabla n_\downarrow)$ is not uniquely defined [15] and a number of different approximations have been proposed [11, 12, 16, 17, 18] for it. Electron density-functional theory is a mature field of condensed matter physics and is widely used in physics, chemistry, engineering and biology, with a large number of reviews and textbooks available [19, 20, 21, 22, 23, 24].

1.2 Classical density functional theory of liquids

The partition function for a classical liquid of N particles in canonical ensemble is

$$Z = \frac{1}{N!}\left(\frac{m}{2\pi\hbar^2\beta}\right)^{3N/2} Z_N$$

where

$$Z_N = \int e^{-\beta V(\vec{r}_1,\vec{r}_2,...,\vec{r}_N)} d\vec{r}_1 d\vec{r}_2 ... d\vec{r}_N$$

where $\beta = 1/kT$ and the Helmholtz free energy is written as

$$F = -kT \log Z$$

Even if we assume that the interaction energy can be written as a sum of pairwise potentials,

$$V(\vec{r}_1, \vec{r}_2, ..., \vec{r}_N) = \sum_{i \neq j} V(\vec{r}_i - \vec{r}_j),$$

the partition function

$$Z_N = \int e^{-\beta \sum_{i \neq j} V(\vec{r}_i - \vec{r}_j)} d\vec{r}_1 d\vec{r}_2 ... d\vec{r}_N$$

is very difficult to evaluate. For any nontrivial $V(\vec{r})$, no analytical solution is known, not even for the case of the hard sphere liquid, where

$$Z_N = \int_{|\vec{r}_i - \vec{r}_j| > d} 1 d\vec{r}_1 d\vec{r}_2 ... d\vec{r}_N.$$

(Here, d is the hard-sphere diameter.)

Because of these difficulties, numerical methods are very important in the study of liquids. The numerical methods are divided in two broad classes. In the first class, each particle is treated individually and statistical averages are done by using either Monte Carlo integration methods or molecular dynamics averages. The second class treats liquid as a continuum medium of density $n(\vec{r})$

$$n(\vec{r}) = \frac{1}{Z_N} \int e^{-\beta V(\vec{r},\vec{r}_2,...,\vec{r}_N)} d\vec{r}_2 ... d\vec{r}_N$$

Continuum theories of liquids were put on a rigorous footing with the introduction of classical density-functional theory [25], which follows from Mermin's [26] generalization of electron density-functional theory for finite temperatures. Application and development of classical density functional theory has blossomed over the last decade. It has seen application in such diverse areas as the study of lattice gasses and adsorption [27, 28, 29, 30, 31], freezing and other phase transitions [32, 33, 34, 35, 36] solid-liquid and liquid-liquid interfaces [37, 38, 39, 40, 41, 42, 43, 44, 45, 46], and polymers [47, 42]. There have been a number of recent reviews [48, 49, 50, 51] and books [52, 53, 54] on the subject as well. The development of this theory proceeds as follows.

In the grand canonical ensemble the equilibrium probability density p_0 for N neutral particles is given by

$$p_0(\vec{r}_1, \vec{r}_2, ..., \vec{r}_N) = \frac{1}{Z} e^{-\beta(V(\vec{r}_1,\vec{r}_2,...,\vec{r}_N)+v_{ext}(\vec{r}_1)+...+v_{ext}(\vec{r}_N)-\mu N)}$$

where μ is the chemical potential and $v_{ext}(\vec{r})$ is the external potential.

If we define the functional

$$\Omega[p] = \mathrm{Tr}_{cl} p(H - \mu N + \beta^{-1} \log p),$$

where $H = V(\vec{r}_1, \vec{r}_2, ..., \vec{r}_N) + v_{ext}(\vec{r}_1) + ... + v_{ext}(\vec{r}_N)$ is the N particle Hamiltonian and

$$\mathrm{Tr}_{cl} = \sum_{N=0}^{\infty} \frac{1}{h^{3N} N!} \int d\vec{r}_1 d\vec{r}_2 ... d\vec{r}_N \int d\vec{p}_1 d\vec{p}_2 ... d\vec{p}_N,$$

analogously to the Hohenberg-Kohn theorem, one can prove [26] that $\min_p \Omega[p]$ is achieved at $p = p_0$ and $\Omega[p_0] = -kT \log Z = \Omega_0$.

The construction of a density-functional theory by constrained search is now

straightforward,

$$\Omega_0 = \Omega[p_0] = \min_p \mathrm{Tr}_{cl} p(H - \mu N + \beta^{-1} \log p) = \tag{1.19}$$

$$\min_{n(\vec{r})} \left(\min_{p->n(\vec{r})} \mathrm{Tr}_{cl} p(V + \beta^{-1} \log p) + \int (v_{ext}(\vec{r}) - \mu) n(\vec{r}) d\vec{r} \right). \tag{1.20}$$

Defining,

$$F[n(\vec{r})] = \min_{p->n(\vec{r})} \mathrm{Tr}_{cl} p(V + \beta^{-1} \log p),$$

we obtain

$$\Omega_0 = \min_{n(\vec{r})} \left(F[n(\vec{r})] + \int (v_{ext}(\vec{r}) - \mu) n(\vec{r}) d\vec{r} \right). \tag{1.21}$$

For interacting systems $F[n(\vec{r})]$ is not known and has to be approximated. The form the non-interacting liquid (ideal gas) is known,

$$F_{id}[n(\vec{r})] = kT \int d\vec{r} n(\vec{r}) (\ln(\lambda^3 n(\vec{r})) - 1),$$

where $\lambda = (h^2 \beta / 2m\pi)^{1/2}$. Note that $F_{id}[n(\vec{r})]$ is a purely local functional of density. Because the interactions in interacting systems generally have a characteristic length scale, fluctuations in the limit of high spatial frequencies do not couple to the enthalpy but only to the entropy, so that $F_{id}[n(\vec{r})]$ captures the effects of the high spatial frequency fluctuations. Thus, the fully interacting functional is customarily written as

$$F[n(\vec{r})] = F_{id}[n(\vec{r})] + F_{ex}[n(\vec{r})].$$

Here, $F_{ex}[n(\vec{r})]$, formally defined as $F[n(\vec{r})] - F_{id}[n(\vec{r})]$, does not couple to high frequency fluctuations so that, for instance, $\delta^2 F_{ex}[n] / \delta n(\vec{r}_1) \delta n(\vec{r}_2)$ is continuous as $\vec{r}_1 \to \vec{r}_2$.

In analogy with electronic density-functionals, one can write for $F_{ex}[n(\vec{r})]$ a local density approximation (LDA), with or without gradient corrections,

$$F_{ex}[n(\vec{r})] = \int d\vec{r} \left(f_0(\vec{r}) + \chi(\vec{r}) (\nabla n(\vec{r}))^2 \right).$$

However, since most liquids are very strongly correlated, neither local or gradient approximation methods prove to be very accurate.

To address the above difficulty, a broad class of "weighted" density approximations [55, 56] for the functional has been used successfully to predict properties of hard sphere liquids and others. In these approximations

$$F_{ex}[n] = \int d\vec{r} n(\vec{r}) \Psi(\bar{n}(\vec{r}))$$

where

$$\bar{n}(\vec{r}) = \int d\vec{r}' w(\vec{r} - \vec{r}'; \tilde{n}(\vec{r})) n(\vec{r}')$$

Two physically acceptable choices for $\tilde{n}(\vec{r})$ are $\tilde{n}(\vec{r}) = n_0$ or $\tilde{n}(\vec{r}) = \bar{n}(\vec{r})$. For either choice, Curtin and Ashcroft [57] present an equation for $w(\vec{r}-\vec{r}')$ whose solution ensures that the theory reproduces the two-point correlation function in the uniform liquid, either only for the density n_0 or for all densities, respectively. For liquids with attractive interactions in general and for water in particular, these equations are known not to allow appropriate solutions [58, 57]. This difficulty can be removed by considering higher order correlations [59]. However, such correlations increase the computational complexity significantly and the required experimental information may not be available. This thesis explores the alternative route of staying with two particle correlations but exploring new functional forms. In particular, Chapter 4 of this thesis introduces a closely related form for $F_{ex}[n]$, which we show always allows solutions of the equation for $w(\vec{r} - \vec{r}')$. This form is

$$F_{ex}[n] = \int d\vec{r} f_{ex}(\bar{n}(\vec{r}))$$

where

$$\bar{n}(\vec{r}) = \int d\vec{r}' w(\vec{r} - \vec{r}; n_0) n(\vec{r}').$$

Bibliography

[1] P. A. M. Dirac, Proceedings of the Royal Society of London. Series A **792**, 714 (1929).

[2] M. C. Payne *et al.*, Rev. Mod. Phys. **64**, 1045 (1992).

[3] J.-L. Fattebert and F. Gygi, Computer Physics Communications **162**, 24 (2004).

[4] T. Biben and D. Frenkel, J. Phys.: Condens. Matter **14**, 9077 (2002).

[5] A. Soper, Chemical Physics **258**, 121 (2000).

[6] J. L. Lebowitz and E. H. Lieb, Phys. Rev. Lett. **22**, 631 (1969).

[7] M. Levy, Phys. Rev. A **26**, 1200 (1982).

[8] P. Hohenberg and W. Kohn, Phys Rev **136**, B864 (1964).

[9] J. E. Harriman, Phys. Rev. A **24**, 680 (1981).

[10] W. Kohn and L. J. Sham, Phys. Rev. **140**, A1133 (1965).

[11] J. P. Perdew and W. Yue, Phys. Rev. B **33**, 8800 (1986).

[12] J. P. Perdew, K. Burke, and M. Ernzerhof, Phys. Rev. Lett. **77**, 3865 (1996).

[13] A. D. Becke, J. Chem. Phys. **96**, 1992 (2155).

[14] J. P. Perdew and Y. Wang, Phys. Rev. B **45**, 13244 (1992).

[15] J. P. Perdew and S. Kurth, *Density Functionals for Non-relativistic Coulomb Systems in the New Century* (Springer-Verlag, Heidelberg, 2003), pp. 1–55.

[16] J. P. Perdew *et al.*, Phys. Rev. B **46**, 6671 (1992).

[17] D. C. Langreth and M. J. Mehl, Phys. Rev. B **28**, 1809 (1983).

[18] J. P. Perdew, Phys. Rev. Lett. **55**, 1665 (1985).

[19] R. G. Parr and W. Yang, *Density-functional theory of atoms and molecules* (Oxford University Press, New York, 1989).

[20] W. Koch and M. Holthausen, *A Chemist's Guide to Density Functional Theory* (Wiley-VCH, Weinheim, 2001).

[21] E. Kaxiras, *Atomic and Electronic Structure of Solids* (Cambridge University Press, Cambridge, UK, 2003).

[22] C. Fiolhais, *A Primer in Density Functional Theory* (Springer, Germany, 2003).

[23] R. M. Martin, *Electronic Structure : Basic Theory and Practical Methods* (Cambridge University Press, Cambridge, UK, 2004).

[24] J. Kohanoff, *Electronic Structure Calculations for Solids and Molecules : Theory and Computational Methods* (Cambridge University Press, Cambridge, UK, 2006).

[25] R. Evans, Advances in Physics **28**, 143 (1978).

[26] N. Mermin, Physical Review **137**, A1441 (1965/03/01).

[27] E. Ustinov, D. Do, and M. Jaroniec, Langmuir **22**, 6238 (2006).

[28] M. B. Sweatman and N. Quirke, Molecular Simulation **31**, 667 (2005).

[29] M. Sweatman and N. Quirke, Langmuir **18**, 10443 (2002).

[30] H. P. Fischer *et al.*, The Journal of Chemical Physics **108**, 3028 (1998).

[31] D. Reinel and W. Dieterich, The Journal of Chemical Physics **104**, 5234 (1996).

[32] M. Valera, F. J. Pinski, and D. D. Johnson, Phys. Rev. E **64**, 062501 (2001).

[33] F. Igloi, G. Kahl, and J. Hafner, Z. Phys. Chem. **156**, 425 (1988).

[34] S. Smithline, ACS Symposium Series **629**, 311 (1996).

[35] H. Graf and H. Löwen, Journal of Physics: Condensed Matter **11**, 1435 (1999).

[36] A. R. Denton and H. Löwen, Journal of Physics: Condensed Matter **9**, 8907 (1997).

[37] A. L. Frischknecht and L. J. D. Frink, Physical Review E (Statistical, Nonlinear, and Soft Matter Physics) **72**, 041924 (2005).

[38] K. Jaqaman, K. Tuncay, and P. J. Ortoleva, The Journal of Chemical Physics **120**, 926 (2004).

[39] K. Johnston and M. W. Finnis, Journal of the American Ceramic Society **85**, 2562 (2002).

[40] J. Reinhard, W. Dieterich, P. Maass, and H. L. Frisch, Phys. Rev. E **61**, 422 (2000).

[41] F. Schmid, Phys. Rev. E **55**, 5774 (1997).

[42] S. Nath, A. Frischknecht, J. Curro, and J. McCoy, Macromolecules **38**, 8562 (2005).

[43] M. C. Stewart and R. Evans, Physical Review E (Statistical, Nonlinear, and Soft Matter Physics) **71**, 011602 (2005).

[44] P. S. Christopher and D. W. Oxtoby, The Journal of Chemical Physics **121**, 5005 (2004).

[45] P. S. Christopher and D. W. Oxtoby, The Journal of Chemical Physics **119**, 10330 (2003).

[46] D. L. Cheung and F. Schmid, The Journal of Chemical Physics **120**, 9185 (2004).

[47] F. Schmid, The Journal of Chemical Physics **104**, 9191 (1996).

[48] D. Henderson, *Fundamentals of Inhomogeneous Fluids* (Marcel Dekker, New York, 1992).

[49] H. Lowen, J. Phys.: Condens. Matter **14**, 11897 (2002).

[50] J. Wu, AIChE Journal **52**, 1169 (2006).

[51] J. K. Percus, Accounts of Chemical Research **27**, 224 (1994).

[52] H. T. Davis, *Statistical Mechanics of Phases, Interfaces and Thin Films* (Wiley-VCH, United States, 1996).

[53] J.-L. Barrat and J.-P. Hansen, *Basic Concepts for Simple and Complex Liquids* (Cambridge University Press, Cambridge, UK, 2003).

[54] J.-P. Hansen and I. McDonald, *Theory of Simple Liquids* (Elsevier, USA, 2006).

[55] S. Nordholm, M. Johnson, and B. Freasier, Australian Journal of Chemistry **33**, 2139 (1980).

[56] P. Tarazona, Molecular physics **52**, 81 (1984).

[57] W. Curtin and N. W. Ashcroft, Phys. Rev. A **32**, 2909 (1985).

[58] S. X. Sun, Phys. Rev. E **64**, 021512 (2001).

[59] C. N. Likos and N. W. Ashcroft, J. Chem. Phys. **99**, 9090 (1993).

Chapter 2

Joint Density-Functional Theory

In this chapter we introduce a new form of density functional theory for the *ab initio* description of electronic systems in contact with a molecular liquid environment. This theory rigorously joins an electron density-functional for the electrons of a solute with a classical density-functional theory for the liquid into a single variational principle for the free energy of the combined system. The theorem that we prove shows that the thermodynamics of a system and its electrons (*solute*) in equilibrium with a liquid environment (*solvent*) can be described rigorously in terms of a *joint density-functional theory* (JDFT) between the electrons in the system and the molecules comprising the solvent. The physics of the equilibrium between a solute and a solvent (cavity formation, dielectric screening, dispersion and repulsion) are then all determined in a single variational principle. Maintaining the first principles nature of density-functional theory, this new approach requires no artificial separation of contributions, no *ad hoc* definitions of cavity shapes, and no empirical fitting of parameters to experimental solvation energies.

A straightforward combination of Mermin's non-zero temperature formulation of density-functional theory[1] with Capitani *et al.*'s extensions of the zero-temperature theory to include nuclear degrees of freedom[2] leads to the following, exact variational principle for the total thermodynamic free energy of an electron-nuclear system in a fixed external electrostatic potential $V(r)$

$$A = \min_{n_t(r),\{N_i(r)\}} \left\{ F[n_t(r),\{N_i(r)\}] + \int d^3r \; V(r) \left(\sum_i Z_i N_i(r) - n_t(r) \right) \right\}, \tag{2.1}$$

where $n_t(r)$ is the thermally and quantum mechanically averaged total single-particle number density of electrons, $N_i(r)$ is the likewise averaged density of the nuclear species i (of atomic number Z_i), and F is a universal functional. (Here, as throughout this work, we employ atomic units, in which Planck's constant and the mass and charge of the electron all have value unity, $\hbar = m_e = e = 1$.) The universality properties of the functional F may be seen directly from its construction within Levy's constrained search procedure[3],

$$F[n_t(r), \{N_i(r)\}] \equiv \min_{\hat{\rho} \to [n_t(r), \{N_i(r)\}]} \mathrm{Tr} \left(\hat{\rho} \hat{H} + k_B T \hat{\rho} \ln \hat{\rho} \right), \tag{2.2}$$

where $k_B T$ is the thermal energy, $\hat{H}$ represents all interactions among and the kinetic energy of the electrons and nuclei, $\hat{\rho}$ is the full quantum-mechanical density matrix for the electron and nuclear degrees of freedom, and the minimization is carried out over only those $\hat{\rho}$ which lead to the given densities $n_t(r)$ and $\{N_i(r)\}$. From this construction it is clear that F, like $\hat{H}$ from which it derives, is independent of the external potential $V(r)$ and depends only upon the identities of the nuclear species i (and, implicitly, upon the temperature T), as Capitani et al.[2] found previously for the case of $T = 0$.

To employ the variational principle Eq. (2.1) in the study of a system to be treated explicitly in contact with a solvent environment, we take the nuclear species i to be those comprising the environment (solvent) and the potential $V(r)$ in Eq. (2.1) to be that arising from the nuclei of the explicit system (solute),

$$V(r) \equiv \sum_I Z_I / |r - R_I|, \tag{2.3}$$

which we take to sit at fixed locations R_I with atomic numbers Z_I. Note that, although we employ a Born-Oppenheimer approximation for the nuclei of the ex-

plicit system, at this stage the treatment of the nuclear species of the environment in Eq. (2.2) is fully quantum mechanical. Thus, Eqs. (2.1,2.2) account for all zero-point motion effects associated with lighter nuclear species in the solvent, such as may be associated with the protons in liquid water or with the helium atoms in superfluid helium when used as a solvent.

Although Eqs. (2.1, 2.2) give a rigorous continuum treatment of the environment nuclei, the variational principle Eq. (2.1) is ultimately impracticable because it requires explicit treatment of all of the electrons, including those associated with the environment. We thus "integrate out" the electrons associated with the environment by writing $n_t(r) = n(r) + n_e(r)$, where $n_e(r)$ is the electron density associated with the environment and $n(r)$ is the electron density associated with the system in contact with that environment. We then perform the minimization over all allowable $n_e(r)$, and finally perform the minimization over all allowable $n(r)$. For this purpose, we define the sets of allowable $n_t(r)$, $n_e(r)$ and $n(r)$ to be all N-representable functions satisfying the criteria of Gilbert[4] and integrating to the appropriate number of electrons for the respective system. Because all thus defined $n_t(r)$ can be constructed as the sum of some allowable $n_e(r)$ and some allowable $n(r)$ and because all such allowable $n_e(r)$ and $n(r)$ sum to an allowable $n_t(r)$, this procedure is guaranteed to recover the final free energy in Eq. (2.1). Thus, we have

$$A = \min_{n(r),\{N_i(r)\}} \left\{ A[n(r),\{N_i(r)\},V(r)] - \int d^3r\ V(r)n(r) \right\} \tag{2.4}$$

where $V(r)$ is defined above in Eq. (2.3) and where

$$A[n(r), \{N_i(r)\}, V(r)] \equiv \min_{n_e(r)} \left\{ F[n(r) + n_e(r), \{N_i(r)\}] + \int d^3r \; V(r) \left(\sum_i Z_i N_i(r) - n_e(r) \right) \right\} \tag{2.5}$$

is universal in the sense that its functional form, like F from which it derives, depends only on the nature of the solvent and, implicitly, the temperature, and that its dependence on the solute is only through the electrostatic potential of the nuclei in $V(r)$. The choice to separate the interaction $-\int d^3r \, V(r)n(r)$ in Eq. (2.4) from the definition of A minimizes the interactions which the unknown functional A must describe, easing the task of finding good approximations. Note, for instance, that with this choice, $V(r)$ in Eq. (2.5) now couples to a neutral charge distribution, thereby minimizing to the greatest extent possible the dependence of A on $V(r)$. All of our systems and subsystems are always charge neutral which is a necessary and sufficient condition for a system to have a thermodynamic limit [5].

Eq. (2.4) gives the exact free energy and exact configuration of the solvent $\{N_i(r)\}$. However, care must be taken in the interpretation of the $n(r)$ which yield the minimum value. The indistinguishability of electrons implies that there can be no fundamentally meaningful assignment of electrons as belonging either to the environment or to the system, and thus no exact formulation can give a unique result for $n(r)$ without some additional prescription. Indeed, for the exact $\{N_i(r)\}$ and any $n(r)$ which integrates to the correct number of electrons and is everywhere less than the exact solution $n_t(r)$ so that $n_e(r) = n_t(r) - n(r)$ is allowable in the above sense, the minimization in Eq. (2.5) will find $n_e(r) = n_t(r) - n(r)$ and thus ultimately produce the exact value for A. There is thus a large set of $n(r)$ which

yield the minimum value in Eq. (2.4), and the variational principle embodied in Eqs. (2.4,2.5) satisfies the fundamental condition of not enforcing any particular, arbitrary decomposition of the total electron density into solvent and environment contributions.

In practice, however, we expect approximations to Eq. (2.5) to break the above degeneracy and to pick out a unique solution. The standard pseudopotential method, which replaces the effects of the nuclei and (relatively) inert core electrons of a solid or molecule with an effective or "pseudo-" potential[6], is in fact an example of an approximation which tracks only a portion of the total electron density and provides results approaching chemical accuracy while suffering no pathologies related to the underlying degeneracy of an apportionment of electrons between two subsystems.

The existence and reliability of so-called "molecular pseudopotential" Hamiltonians [7, 8, 9] implies the existence of reliable approximations to Eq. (2.5) which pick out a unique solution for $n(r)$. Such pseudopotential Hamiltonians replace the effects of the nuclei and electrons of a collection of molecules on the electrons of an external system (solute) with an effective potential $V_{\{R_i\}}(r)$, which depends explicitly on the locations of the molecular nuclei $\{R_i\}$. Such Hamiltonians have proved to be quite accurate. Using them, for instance, Vaidehi *et al.* find the solvation energy of Li^+ to within 0.6 kcal/mole, and Kim, Park and co-workers find results for total energies with an accuracy acceptable for the study of the problem of an excess electron solvated in water.

Formulating the exact thermodynamics of such Hamiltonians with the same approach that leads to Eq. (2.1) gives directly the principle in Eq. (2.4), but now

with

$$A[n(r),\{N_i(r)\},V(r)] \equiv \min_{\hat{\rho}\to[n(r),\{N_i(r)\}]} \mathrm{Tr}\ \left(\hat{\rho}\hat{H}_{\{R_i\},\{R_I\}} + k_B T\hat{\rho}\ln\hat{\rho}\right), \tag{2.6}$$

where $n(r)$ represents the electron density associated with the solute alone and $\hat{H}_{\{R_i\},\{R_I\}}$ represents the internal electron gas Hamiltonian for the solvent electrons *alone*, the interaction of these electrons with the molecular pseudopotential $V_{\{R_i\}}(r)$ and a model potential function $U(\{R_i\},\{R_I\})$ describing the interactions among the environment molecules and the interaction between those molecules and the nuclei of the solute through the electrostatic potential $V(r)$ defined in Eq. (2.3). Because the electrons have been already apportioned between the solute and the solvent during the construction of $\hat{H}_{\{R_i\},\{R_I\}}$, the functional A in Eq. (2.6) represents an example of an approximation to Eq. (2.5) which is both reliable and free of any potentially pathological issues associated with degenerate solutions for $n(r)$. With the functional dependence of A established in Eq. (2.4), we next separate out known components and leave an unknown part to be approximated,

$$\begin{aligned} A[n(r),\{N_i(r)\},V(r)] &\equiv A_{KS}[n(r)] \\ &+ A_{lq}[\{N_i(r)\}] + U[n(r),\{N_i(r)\},V(r)], \end{aligned} \tag{2.7}$$

where $A_{KS}[n(r)]$ is standard universal Kohn-Sham electron-density functional of the explicit system when in isolation, $A_{lq}[\{N_i(r)\}]$ is the "classical" density functional for the liquid solvent environment when in isolation, and $U[n(r),\{N_i(r)\},V(r)]$, defined formally and exactly as the difference between the exact functional and the sum of the two former functionals, is a new functional describing the coupling between the systems. The new functional $U[n(r),N(r),V(r)]$ has the same universality properties as the functional A from which it derives.

Bibliography

[1] N. D. Mermin, Phys. Rev. **137**, A1441 (1965).

[2] J. Capitani, R. Nalewajski, and R. Parr, J. Chem. Phys. **76**, 568 (1982).

[3] M. Levy, Proceedings of the National Academy of Sciences of the United States of America **76**, 6062 (1979).

[4] T. Gilbert, Phys. Rev. B **12**, 2111 (1975).

[5] J. L. Lebowitz and E. H. Lieb, Phys. Rev. Lett. **22**, 631 (1969).

[6] M. Payne *et al.*, Rev. Mod. Phys. **64**, 1045 (1992).

[7] N. Vaidehi, T. Wesolowski, and A. Warshel, J. Chem. Phys. **97**, 4264 (1992).

[8] K. S. Kim *et al.*, Phys. Rev. Lett. **76**, 956 (1996).

[9] I. Park *et al.*, Computational Materials Science **21**, 291 (2001).

Chapter 3

Joint Density-Functional Theory: *Ab Initio* Study of Cr_2O_3 Surface Chemistry in Solution

Ab initio calculations have shed light on many physicochemical questions, including chemical reactions in solution and chemical reactions at surfaces [1, 2, 3]. Although computational chemistry is now able to provide not only qualitative but also quantitative insights into surface chemistry [2], so far these studies have been limited to reactions in a vacuum, even though, experimentally, these reactions often occur in solvent environments. A fundamental roadblock to *ab initio* study of surface reactions in solution is that current continuum approaches do not sit on a firm theoretical foundation.

Using the new form of density-functional theory for the *ab initio* description of electronic systems in contact with a molecular liquid environment introduced in Chapter 2, we present a detailed study of the impact of a solvent on the surface chemistry of Cr_2O_3, the passivating layer of stainless steel alloys. In comparison to a vacuum, we predict that the presence of water has little impact on the adsorption of chloride ions to the oxygen-terminated surface but has a dramatic effect on the binding of hydrogen to that surface. These results indicate that the dielectric screening properties of water, which arise from reorientation of dipole moments on water molecules around the charged particle, are important to the passivating effects of the oxygen-terminated surface.

3.1 Introduction

Each year, corrosion costs the United States $276 billion, [4] approximately 3.1% of the gross domestic product, and many approaches have been used to understand and model this complex process [5, 6, 7]. High-performance stainless steel alloys contain chromium resulting in the formation of a Cr_2O_3 passivating surface layer, which provides corrosion resistance. Even with this layer, such alloys are susceptible to breakdown in acidic, chlorine-containing, aqueous environments,[8, 9] the study of which demands simultaneous treatment of surfaces, reactants and the aqueous dielectric environment. Direct experiments are difficult, and although *ab initio* calculations have a history of answering many such questions, to date they have not been able to address the effect of the solvent on surface reactions. Alavi *et al.*,[10] for instance, have studied the adsorption of HCl on single-crystal α-Al_2O_3 (0001) surfaces and calculated adsorption energies as a function of surface coverage within density-functional theory, but all of their results are obtained in a vacuum environment.

Previous studies of Cr_2O_3 have been limited to pure surfaces in vacuum [11], an unrealistic environment for the study of corrosion. These studies indicated that the highest occupied and lowest unoccupied molecular orbitals (HOMOs and LUMOs) are localized on the chromium ions, suggesting that the oxygen-terminated surface could provide a stable barrier against acidic chlorinated environments *if* the surface oxygen layer could be prevented from reacting with species in the solution. In this chapter we put forth evidence to support the novel hypothesis that the dielectric screening effects associated with an aqueous environment actually prevent the formation of bonds with aqueous species such as protons, thereby rendering the oxygen-terminated surface virtually nonreactive.

Models for calculating solvation energies from continuum dielectric theory[12] have been applied to single molecules or activated complexes but not to molecules adsorbed on surfaces, perhaps because such methods are generally applied to molecules. Here, we build an approach to *ab initio* calculations in a continuum dielectric environment which sits on the theoretical foundation of Chapter 2. Below, we show that this new approach, which in a simple approximation is related to that recently introduced by Fattebert and Gygi[13], gives results in good agreement with currently accepted quantum chemical methods and is well-suited to surfaces. Finally, we apply the approach to carry out the first *ab initio* study of the reactivity of hydrogen and chlorine on an oxygen-terminated $Cr_2O_3(0001)$ surface in contact with a solution.

3.2 Theoretical approach: joint density-functional theory

Because of the large cells required in this study (well over one hundred atoms), the only practicable *ab initio* approach suited to describe the electrons of the surface and the reactants is the density-functional theory.[11] The size of the surface cell and time-scales needed for proper thermodynamic averaging make a direct molecular dynamics treatment of the aqueous environment infeasible, thus raising the question of how to treat the solvent. To do so within a rigorous framework, we use the concept of a *joint density-functional theory* (JDFT) between the electrons in the surface and the molecules comprising the solvent, introduced in Chapter 2.

This new theory affords the opportunity to maintain a density-functional treatment of the electrons of the system of interest while giving a rigorous description of the solvent in terms of "classical" density-functional theories[14], which treat water rigorously in terms of a simple thermodynamically averaged molecular density and

a functional to which computationally tractable approximations are known[15].

While the availability of classical density-functional approximations to A_{lq}[15] makes Eq. (2.7) an attractive starting point for future work, in this first work, we make the further simplification of performing the minimization over $\{N_i(r)\}$, resulting in the variational principle

$$A = \min_{n(r)} \left(A_{KS}[n(r), \{Z_I, R_I\}] - \int d^3r \; V(r)n(r) + W[n(r), \{Z_I, R_I\}] \right), \quad (3.1)$$

where

$$W[n(r), \{Z_I, R_I\}] \equiv \min_{\{N_i(r)\}} (A_{lq}[\{N_i(r)\}] + U[n(r), \{N_i(r)\}, \{Z_I, R_I\}])$$

is universal in the sense that its functional form depends solely upon the identity of the environment (and, implicitly, the temperature). Note that, in principle, the theory at this stage is exact. Below we outline the models and approximations which we introduce because the exact forms of the functionals $A_{KS}[n(r), \{Z_I, R_I\}]$ and $W[n(r), \{Z_I, R_I\}]$ are unknown.

3.3 Computational details

For treatment of the electrons in the chromium-oxide surface through the functional $A_{KS}[n(r), \{Z_I, R_I\}]$, we apply the standard local spin-density approximation (LSDA)[16]. The calculations themselves employ the total-energy plane-wave density-functional pseudopotential approach[17] with potentials of the Kleinman-Bylander form[18] with p and d nonlocal corrections at a cutoff of 40 hartrees. Supercells with periodic boundary conditions in all three dimensions represent the surfaces of isolated oxygen-terminated (0001)-oriented slabs of Cr_2O_3 of thickness 13 Å separated by 7.8 Å of either vacuum or solvent. The in-plane boundary

conditions suffice to describe 2×2 reconstructions and consist of four times the unit from Cline *et al.*[11] so as to allow sufficient isolation of solvent volumes excluded by chlorine adsorbed on the surface. The supercell contains a total of 40 chromium and 72 oxygen atoms with chlorine or hydrogen added to the two surfaces in inversion-symmetric pairs, one on each side of the slab. Finally, we use a single k-point to sample the Brillioun zone of the surface slab, which corresponds precisely to the sampling density previously established by Cline *et al.*[11]. Those authors established that for this choice of functional, pseudopotential, plane-wave cutoff, sampling density in the Brillioun zone and supercell, calculations give a good description of the bulk and surface properties of Cr_2O_3. As in the aforementioned work, we employ the analytically continued functional approach[17, 19] to minimize the Kohn-Sham energy with respect to the electronic degrees of freedom. Below, we relax all ionic configurations until the total energy is within 0.027 eV of the minimum and the maximum force in any direction is less than 0.3 eV/Å.

3.4 Local dielectric theory

For the environment functional $W[n(r), \{Z_I, R_I\}]$ in Eq. (3.1), we take the interaction of the electron and nuclear charges of the system under study with a dielectric environment in which the dielectric constant is local in space and has a value dependent only upon the electron density at each point, $\epsilon(r) \equiv \epsilon(n(r))$. This corresponds to taking the primary mode of interaction between the system and the environment to be long-range screening associated with favorable alignment of the dipole moments of the water molecules with the instantaneous electrostatic field of the system under study. In reality, correlations among water molecules imply that the true dielectric response function $\epsilon(r, r')$ is non-local in space, a simplifi-

cation which we we shall relax somewhat in Chapter 4. For now, we focus on the long wave-length ($k \to 0$) dielectric response and so approximate $\epsilon(r, r')$ as a local function $\epsilon(r)$. The dependence of the value of $\epsilon(r)$ on the local density $n(r)$ in our model allows us to eliminate dielectric screening due to the environment from the interior regions of the system under study. Thus, in effect, we have in this simple model a dielectric cavity around our system determined by isosurfaces of system's electron density.

Taking in this way the dielectric interaction to be the most significant and modeling it with a local approximation to the dielectric constant is standard practice in semiempirical quantum-chemical continuum dielectric models[20] but does not take direct account of molecular-scale effects such as changes in the dielectric response near the surface due to effects like hydrogen bonding with the surface. As noted above, writing the dielectric constant as a function of the explicit electron density allows the electronic structure to determine the boundary between the solvent environment and the explicit system, an approach which Fattebert and Gygi have shown to reproduce well results from the quantum chemistry literature[13]. For a more detailed calculation in the future, one could improve upon our results by including a small number of water molecules explicitly at the surface of the system or by employing the more detailed variational principle of Eq. (2.7) with approximate functionals which account for nonlocal dielectric effects as well as surface tension associated with the solid-liquid interface.

In practice, we implement the above model for W by computing the total free energy of the system in contact with the environment as the stationary point with

respect to both the electrons and the mean electrostatic field $\phi(r)$ of the functional

$$\begin{aligned} A &= A_{TXC}[n_\uparrow(r), n_\downarrow(r)] + \Delta V_{ps}[n_\uparrow(r), n_\downarrow(r)] \\ &\quad - \int d^3r \left\{ \phi(r) \left(n_{tot}(r) - \sum_I Z_I \delta^{(3)}(r - R_I) \right) - \frac{\epsilon(n(r))}{8\pi} |\nabla\phi(r)|^2 \right\} \end{aligned} \tag{3.2}$$

where $n_\uparrow(r)$, $n_\downarrow(r)$ and $n_{tot}(r)$, respectively, are the up-, down-, and total electron densities, $A_{TXC}[n_\uparrow(r), n_\downarrow(r)]$ is the Kohn-Sham single-particle kinetic plus exchange correlation energy within the local spin-density approximation, ΔV_{ps} is the difference in the total pseudopotential energy from that expected from pure Coulombic interactions with point ions of valence charges Z_I at locations R_I, and $\delta^{(3)}(r)$ is the three-dimensional Dirac-δ function. Note that, although we do work directly with the Kohn-Sham orbitals, for brevity we have written the above in terms of the electron densities. We also note that at this level of approximation our joint density-functional theory takes the same form as the approach of Fattebert and Gygi[13], which introduced the form as a computational device without formal justification. Finally, we were able to implement this approach with relatively modest changes to our group's preexisting density-functional software. The primary change was to combine the calculation of the Hartree field (potential from the electrons) and the ionic potential (local part of the ionic pseudopotential) into a single solution of Poisson's equation in the presence of the dielectric function $\epsilon(n(r))$.

For the local dielectric function $\epsilon(n(r))$, we choose a specific form which varies smoothly from the dielectric constant of the bulk solvent ϵ_b when the electron density $n(r)$ is less than a critical value n_c indicative of the interior of the solvent to the dielectric constant of vacuum $\epsilon = 1$ when $n(r) > n_c$. Specifically, we take

$$\epsilon(n) = 1 + \frac{\epsilon_b - 1}{2} \operatorname{erfc}\left(\frac{\ln(n/n_c)}{\sqrt{2}\sigma} \right), \tag{3.3}$$

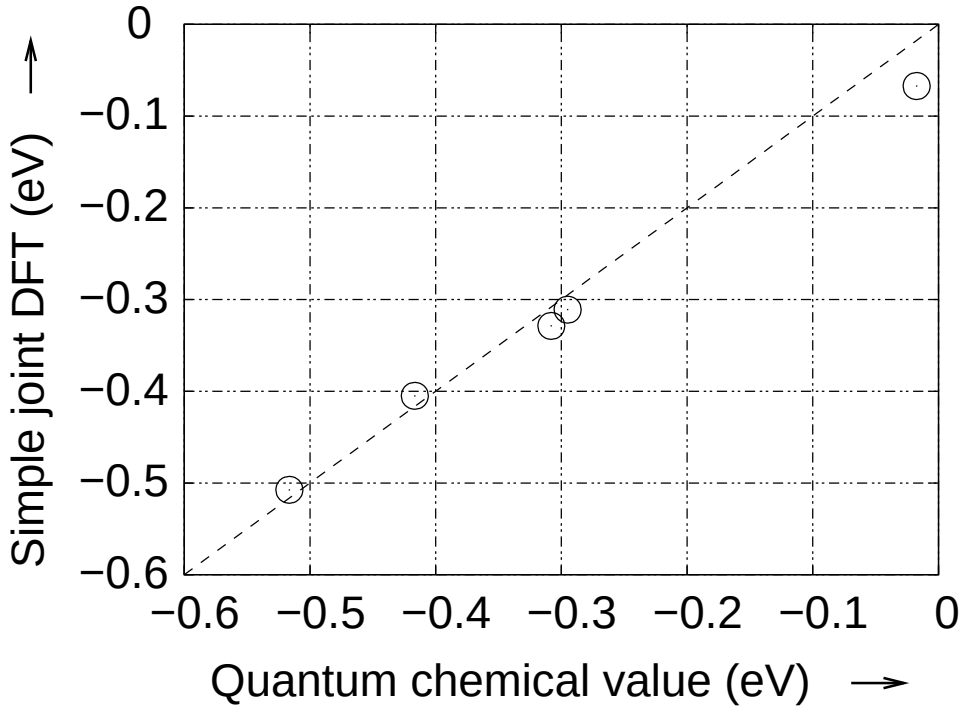

Figure 3.1: Comparison of the predictions of a simple joint density-functional theory (vertical axis) with established quantum chemical values (horizontal axis) for the electrostatic contribution to the solvation energy of acetamide, acetic acid, methanol, ethanol and methane (from left to right) from Marten *et al.*[21].

where the parameter σ, to which the results are not very sensitive, controls the width of the transition from bulk to vacuum behavior. (Note that Fattebert and Gygi[13] have introduced and justified a very similar form to model $\epsilon(n)$.) To determine the parameters σ and n_c for this simple model, we fit computed electrostatic solvation energies in aqueous solution ($\epsilon_b = 80$) to the accepted values from the quantum-chemical literature for methane, ethanol, methanol, acetic acid and acetamide[21]. Figure 3.1 summarizes the quality of this comparison for our final choice of fit parameters, $\sigma = 0.6$ and $n_c = 4.73 \times 10^{-3}$ Å^{-3}.

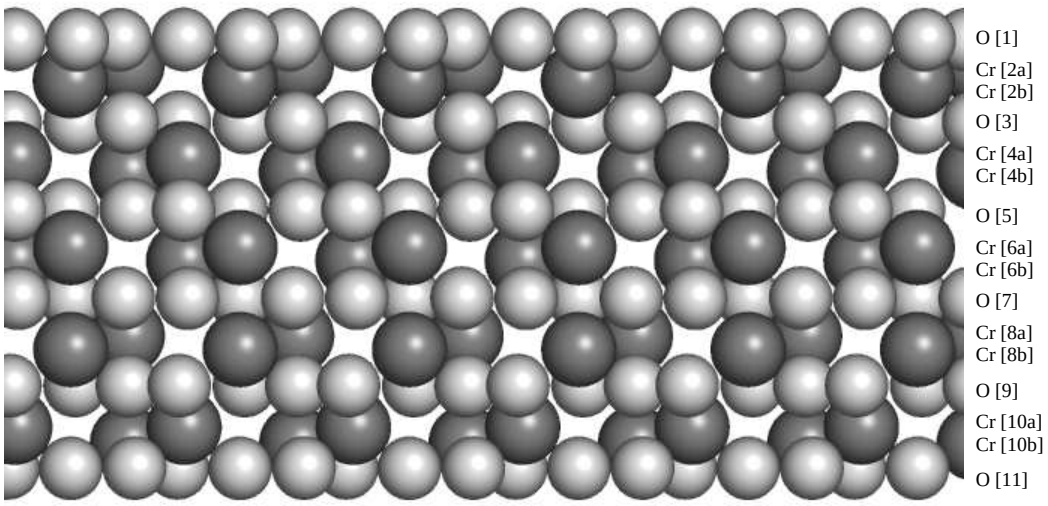

Figure 3.2: Relaxed structure of a pristine surface slab, side view ([0001] direction runs vertically up the page): oxygen (light gray spheres), chromium (dark gray spheres). The labeling of atomic layers follows Cline *et al.*[11].

3.5 Results and discussion

3.5.1 Pristine surface

Cline *et al.*[11] review in detail the structure of bulk Cr_2O_3 and the relaxation of its pristine (0001) oxygen-terminated surface. Figure 3.2 shows the relaxed structure of our supercell surface slab. The bulk structure consists of alternating planar layers of oxygen atoms separated by bilayers of chromium. As Cline *et al.*[11] also find, the primary relaxation associated with forming the surface is for the oxygen-terminated surface layers to move inward toward the bulk crystal with slight in-plane displacements.

Figure 3.3a.1 shows the filled and empty energy levels from our supercell calculation of the (0001) oxygen-terminated surface of Cr_2O_3 in a vacuum environment. Following standard practice, we choose the zero of energy to be the Fermi level, the energy below which states are fully occupied and above which they are empty. The states at the zero line in the figure are thus the highest occupied molecular orbitals (HOMOs) and the first states above the line are the lowest unoccupied molecular orbitals (LUMOs). The figure shows the levels of the pristine surface to be fully filled up to a gap of about 0.5 eV separating the HOMOs and LUMOs.

To provide a more global view, Figure 3.4 presents the *intensive* density of states, the number of levels from Figure 3.3a.1 per unit energy *per electron* as a function of energy, computed using a Gaussian broadening of width σ=0.41 eV. To underscore the distinction between occupied and unoccupied states, the figure gives a separate curve for each. Finally, as a guide to the identification of the bands, the figure also contains markers for the LSDA atomic eigenvalues of oxygen and chromium, which have been shifted uniformly upward by 4.4 eV to approximately counteract the shifting of the Fermi level of the supercell states to zero energy. Although there may be no *a priori* reason to expect neutral atomic eigenvalues to be relevant for this ionic system, we find below that detailed inspection of the corresponding local densities indicates that the features in the density of states correspond precisely in spin orientation, localization, and orbital character to those of the nearby atomic states indicated in the figure.

Three features in the supercell density of states play important roles in the chemistry of this surface. First, the highest occupied *oxygen* orbitals appear as the shoulder (from $\sim$-4 eV to $\sim$-2 eV) of the oxygen $2p$ band, which consists of "minority" spin electrons, electrons with spin opposite to the net atomic spin.

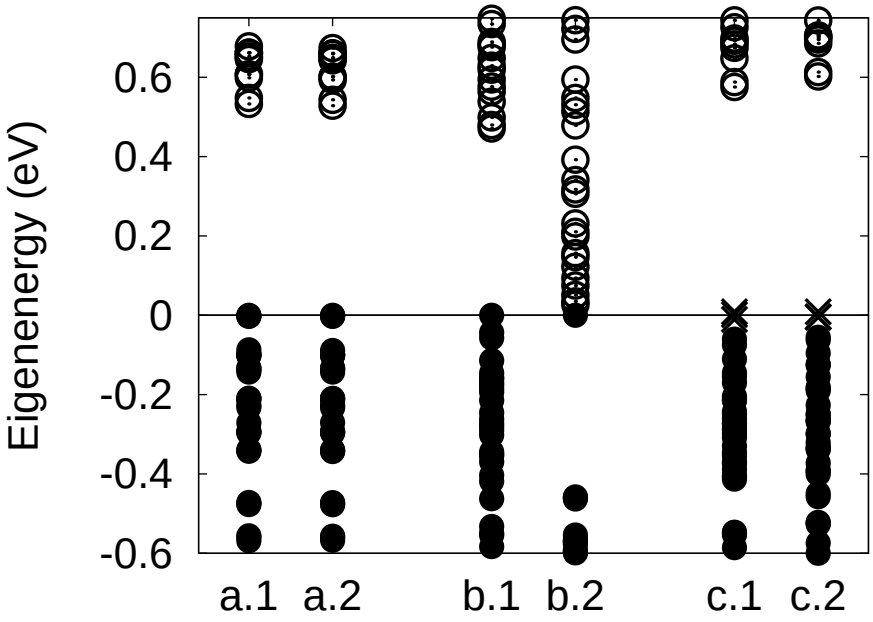

Figure 3.3: Near-gap energy levels for (a) pristine, (b) hydrogenated, and (c) chlorinated system in (1) vacuum and (2) dielectric: filled levels (solid circles), empty levels (open circles), and partially filled levels (crosses).

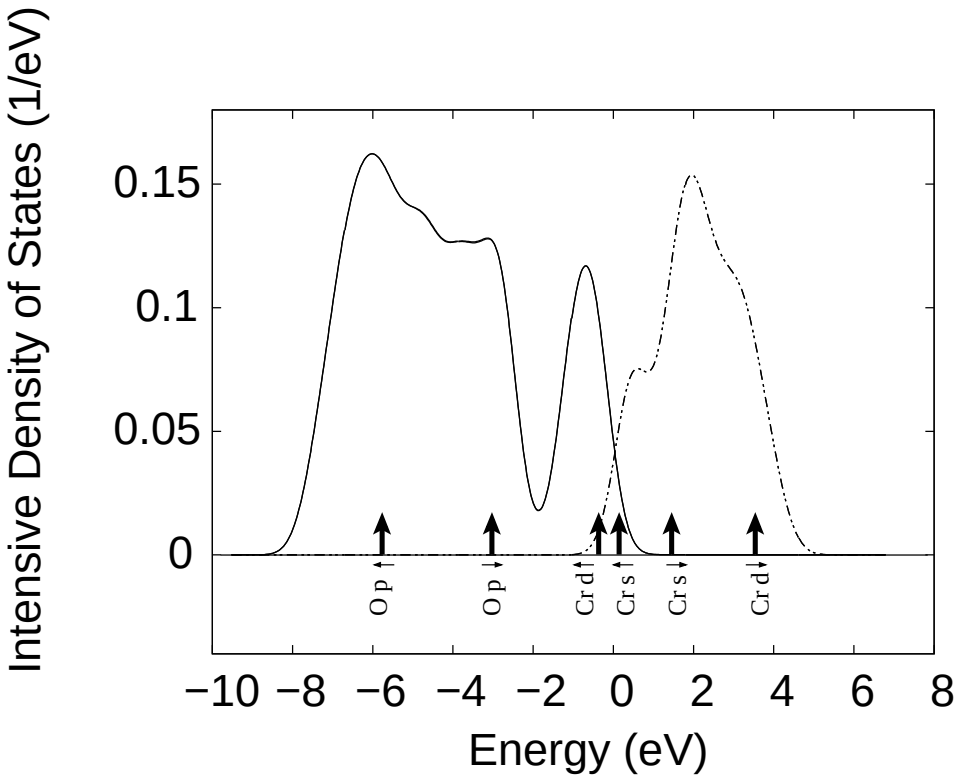

Figure 3.4: Total density of states per electron of pristine supercell slab in vacuum (solid curve) and in solution (virtually indistinguishable dashed curve): occupied states (curve on left), unoccupied states (curve on right), and LSDA atomic eigenvalues (vertical arrows) labeled according to alignment (↑) or anti-alignment (↓) with direction of net atomic spin.

Figure 3.5a presents the sum of the probabilities associated with states in this range and clearly indicates this shoulder to be a surface oxygen band. (The contour level in this and all subsequent electron density maps is set at the same value of 0.68 $e^-/\text{Å}^3$, chosen so as to make evident the localization and orbital character of the corresponding states.) The localization of different spin types to either surface corresponds to the fact that the oxygen atoms on each surface have opposite net spin direction. Next, the highest occupied molecular orbitals (HOMOs) overall appear as an *sd*-hybrid chromium band (from ∼-2 eV to ∼0 eV) consisting of electrons of "majority" spin, spin aligned with the net atomic spin. Figure 3.6 shows these states to be *bulk* chromium states, with atoms alternating in majority spin direction corresponding to the anti-ferromagnetic nature of the bulk material. Finally, the LUMOs of the system appear as the low energy majority spin shoulder (from ∼0 H to ∼1 eV) of an empty chromium band. Figure 3.7 shows this shoulder to consist of surface states of primarily chromium character protected under the outer oxygen layer. This character of the HOMOs and LUMOs suggests that any oxygen missing from the outer surface would expose a reactive chromium layer underneath.

Upon repeating the pristine surface calculation in the presence of a dielectric environment, we find virtually no change. There is no change in Figure 3.2 and, although some very small changes are evident in going from Figure 3.3a.1 to Figure 3.3a.2, the global picture of the density of states in Figure 3.4 is visually indistinguishable for vacuum (solid curve) and dielectric (dashed curve). Finally, inspection of density maps corresponding to Figures 3.5–3.7 again shows no noticeable changes.

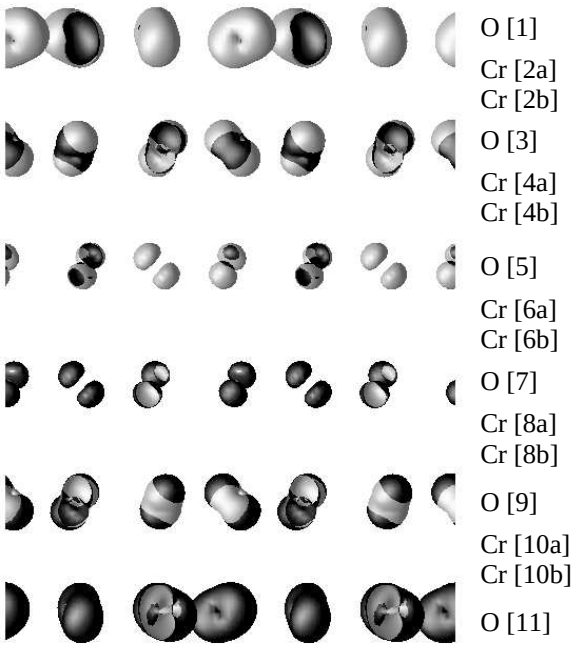

Figure 3.5: Contour level ($0.68\ e^{-}/\text{Å}^3$) of the sum of probability densities from the highest energy shoulder of the oxygen $2p$ band, side view ([0001] direction runs vertically up the page): up spin (black surface), and down spin (white surface). Locations of atomic layers are indicated as in Figure 3.2.

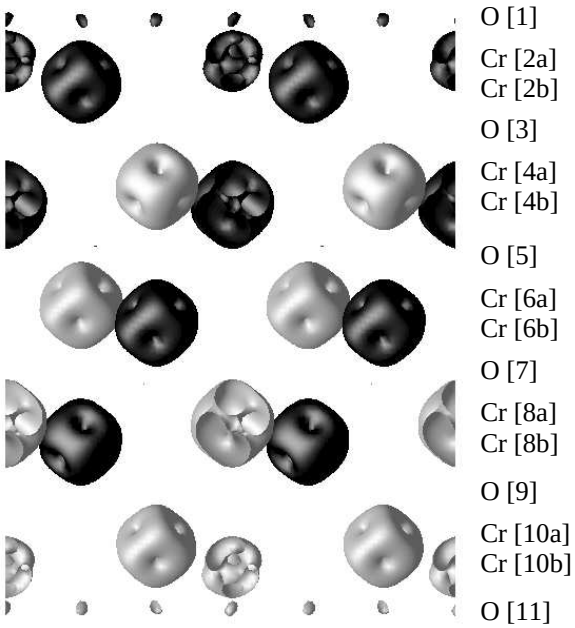

Figure 3.6: Contour level ($0.68\ e^{-}/\text{Å}^3$) of sum of probability densities from the chromium $sd\uparrow$ band, side view ([0001] direction runs vertically up the page): up spin (black surface), and down spin (white surface). Atomic layers indicated as in Figure 3.2.

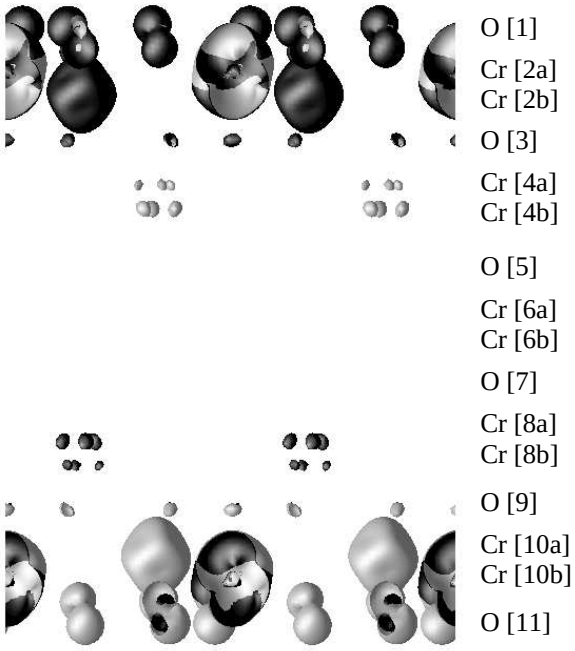

Figure 3.7: Contour level $(0.68\ e^{-}/\text{Å}^3)$ of sum of probability densities from the lowest energy shoulder of the chromium $sd \downarrow$ spin band, side view ([0001] direction runs vertically up the page): up spin (black surface), down spin (white surface). Atomic layers indicated as in Figure 3.2.

3.5.2 Interaction with hydrogen

Anticipating bonding with oxygen, we initially placed a hydrogen atom in vacuum directly on top of one of the surface oxygen atoms, all of which are equivalent by symmetry. Figure 3.8a shows that, upon relaxation, the hydrogen atom cants away from the surface perpendicular while appearing to form a bond with the underlying oxygen atom: the final relaxed O-H distance is 0.95 Å, quite close to the experimental O-H separation in H_2O (0.96 Å). Figure 3.9 shows that the canting of the hydrogen atom is in the same direction as one would expect for the $2p$ orbital of the associated oxygen atom given its in-plane displacement. Finally, Figure 3.10a, which shows the total electron density associated with the chemisorbed H, confirms the presence of the bond as a small protrusion in the density near the hydrogen atom.

Figure 3.3b.1 shows the filled and empty energy levels of the hydrogenated surface in a vacuum environment. As with the pristine surface (Figure 3.3a), the energy levels are fully filled up to a HOMO-LUMO gap, consistent with the observed bonding. To better resolve the bond associated with the chemisorbed hydrogen, Figure 3.11 presents the *local* density of states in the vicinity of the hydrogen atom, which we compute in the same way as the total density of states of Figure 3.4 but by now weighing each level with the probability of an electron in the level being within 0.69 Å of the proton. The local density of states shows that the hydrogen atom interacts mostly with the surface oxygen $2p$ band. A plot of the total density associated with this surface band, Figure 3.12a, confirms that it contains most of the density protrusion associated with the O-H bond. Finally, Figure 3.13a shows that the HOMO of the hydrogenated surface, while maintaining significant bulk chromium character, indeed localizes near the hydrogen atom.

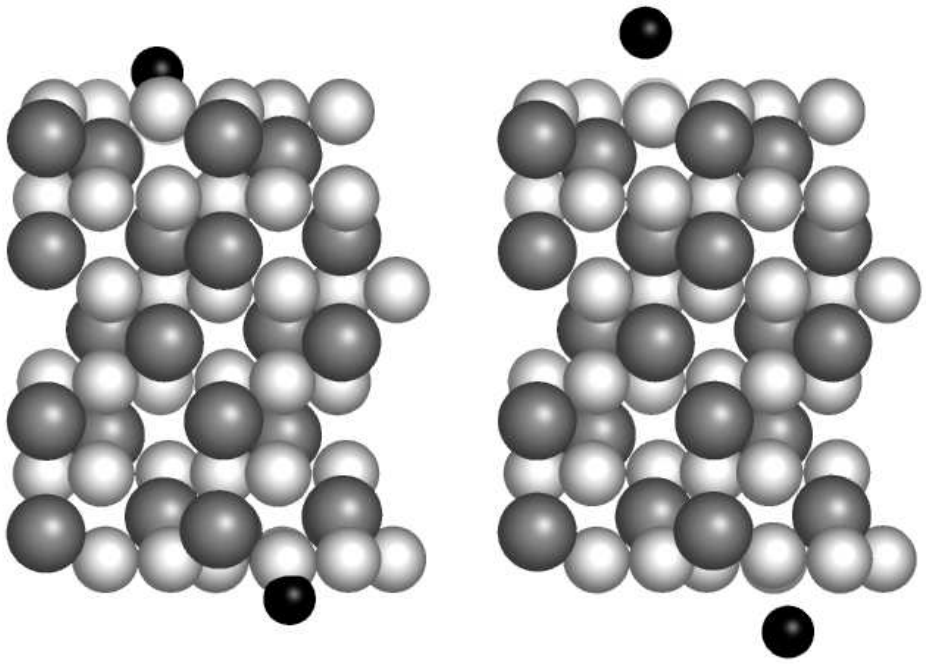

(a) (b)

Figure 3.8: Relaxed structure of surface slab with adsorbed hydrogen in (a) vacuum and (b) dielectric: oxygen (light gray spheres), chromium (dark gray spheres), and hydrogen (black spheres). Same view as Figure 3.2 but showing atoms from a single supercell.

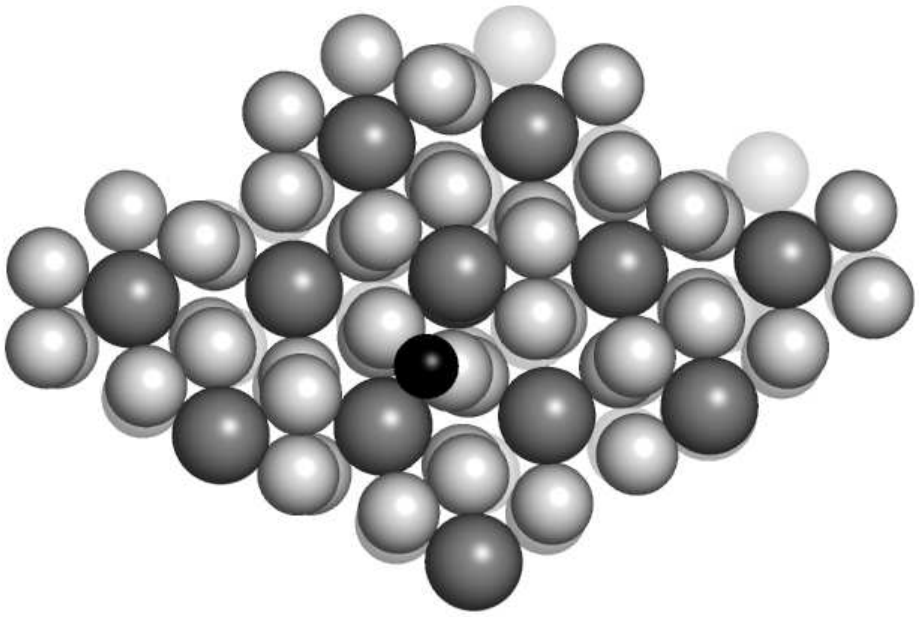

Figure 3.9: Relaxed structure of a single supercell with adsorbed hydrogen in vacuum, top view ([0001] direction normal to page): oxygen (light gray spheres), chromium (dark gray spheres), and hydrogen (black sphere).

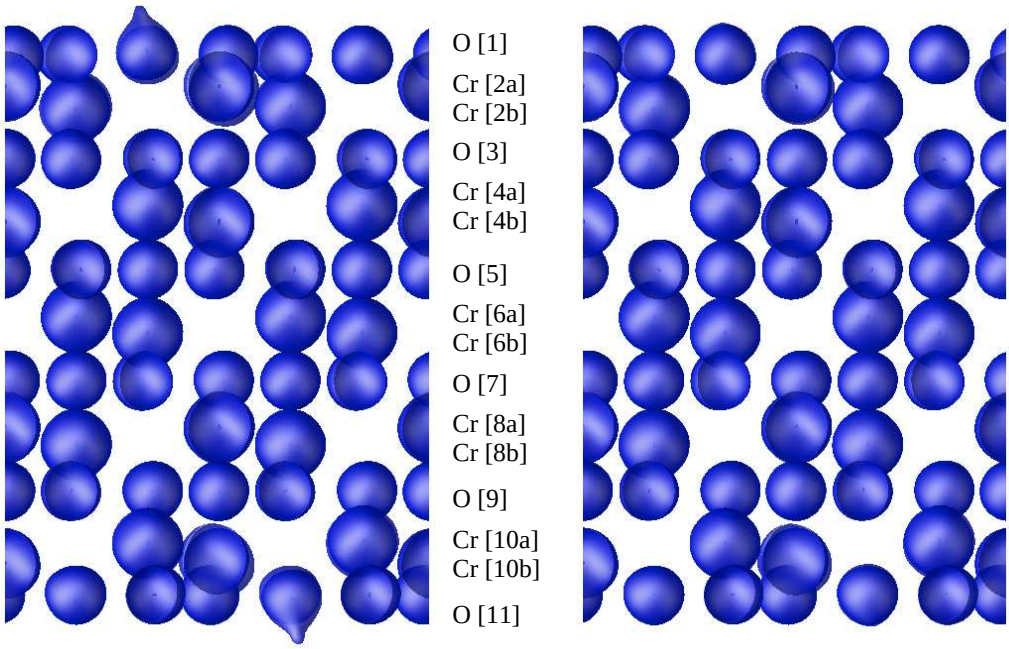

(a) (b)

Figure 3.10: Contour level ($0.68\, e^{-}/\text{Å}^3$) of total electron density for hydrogen atom adsorbed on oxygen-terminated (0001) surface in (a) vacuum and (b) dielectric, side view ([0001] direction runs vertically up the page). Atomic layers indicated as in Figure 3.2. Note that most contours are near spherical and appear as balls centered on atoms.

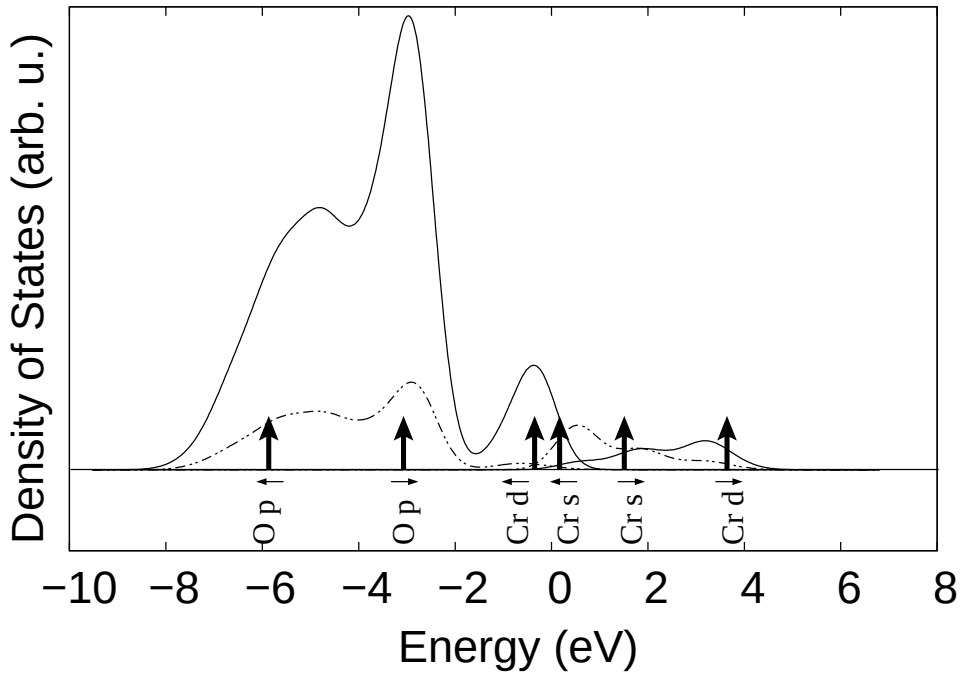

Figure 3.11: Local density of states within 0.69 Å of the proton for hydrogen interacting with oxygen-terminated (0001) surface in vacuum (solid curve) and solution (dashed curve). Same conventions as Figure 3.4.

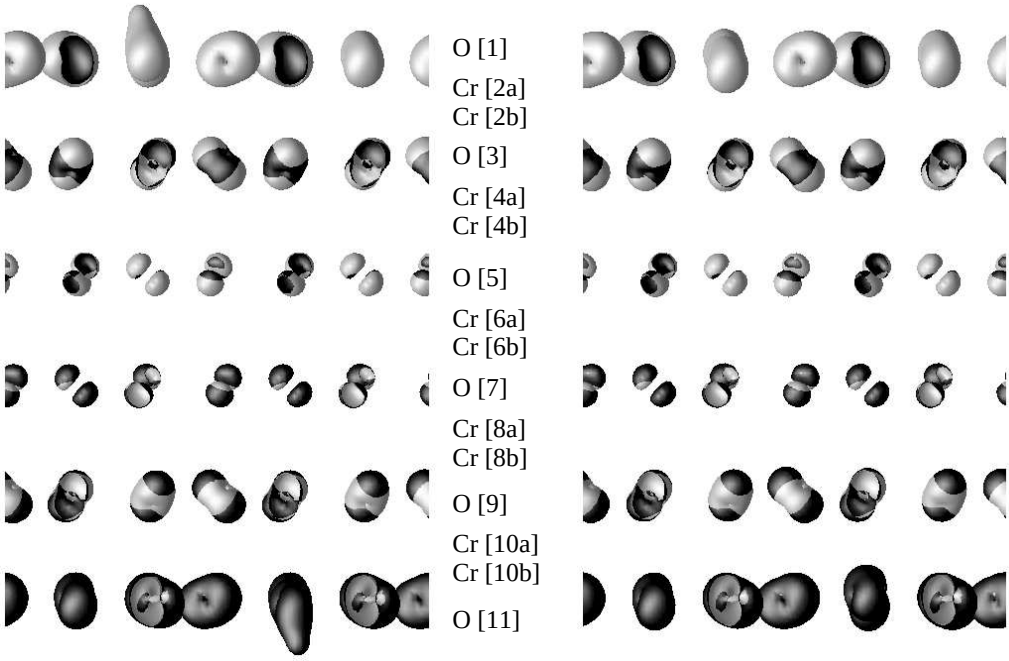

(a) (b)

Figure 3.12: Contour level ($0.68\ e^-/\text{Å}^3$) of the sum of probability densities associated with oxygen $2p$ surface band in (a) vacuum and (b) dielectric: up spin (black surface), down spin (white surface). Atomic layers indicated as in Figure 3.2.

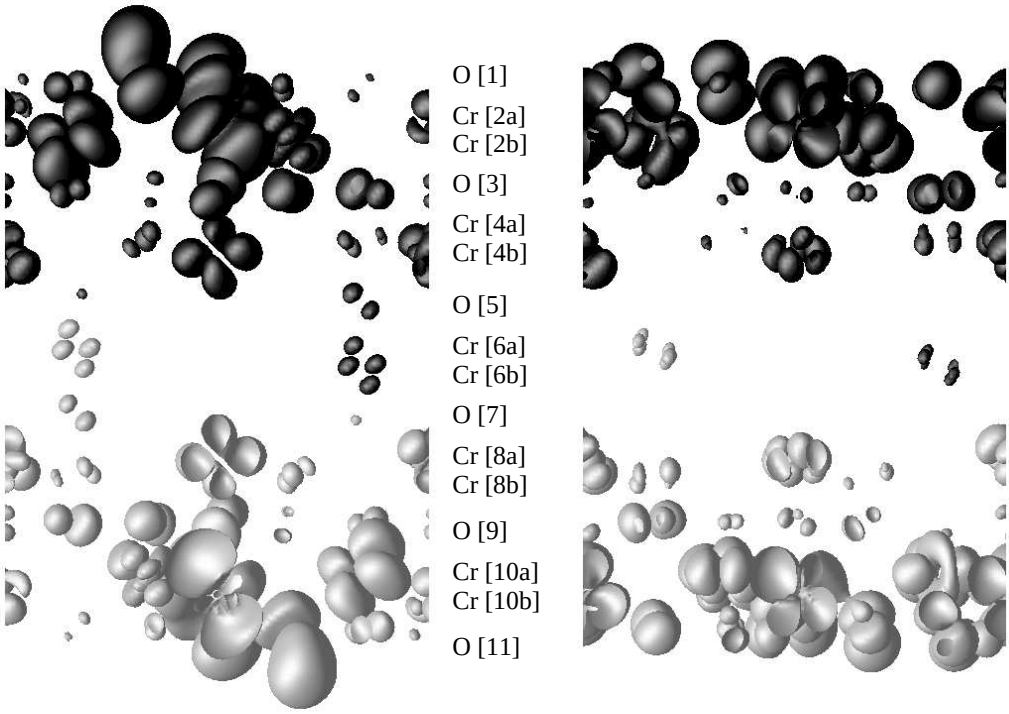

(a) (b)

Figure 3.13: Contour level (0.68 $e^{-}/\text{Å}^3$) of the HOMO of hydrogen interacting with the oxygen-terminated (0001) surface in (a) vacuum and (b) dielectric, side view ([0001] direction runs vertically up the page): up spin (black surface), down spin (white surface). Atomic layers indicated as in Figure 3.2.

To determine the final atomic configuration in the presence of a solvent, we begin with the positions from Figure 3.8a and relax the atomic coordinates within the approximate joint density functional of Eqs. (3.2,3.3) until the maximum force on any atom is less than 0.3 eV/Å. Figure 3.8b, which displays the resulting configuration, shows that the presence of the dielectric has a dramatic effect on the hydrogen. The nearest oxygen-hydrogen distance has increased to 2.3 Å, clearly breaking the O-H bond and returning the hydrogen atom to the solution. Consistent with this picture, the largest residual force remains on the hydrogen atom in the direction tending to push it yet further from the surface. Lack of any indication of the presence of the hydrogen atom in the resulting total charge density, Figure 3.10b, indicates that the atom enters the solution as an ion.

Figure 3.3b.2 shows that upon the removal of the proton from the surface, the excess electron from the O-H bond appears simply as a donated conduction electron just above the energy gap. Consistent with this donation, the dashed curve in Figure 3.11 shows a dramatic reduction in the local density of states near the proton, and the HOMO in Figure 3.13b now shows more of the surface chromium character of the original LUMO band from Figure 3.7.

3.5.3 Interaction with chlorine

Anticipating the possibilities of ionic bonding for chlorine, we initially placed (in the 1×1 surface supercell) a chlorine atom in vacuum directly above each of the two distinct types of Cr^{3+} site from the outermost chromium bilayer and found the site above the innermost of the two component layers to be favored by 0.4 eV. Figure 3.14 shows a top ([0001]) view of the relaxed configuration for this site when computed within the 4×4 supercell. We find relatively little relaxation from

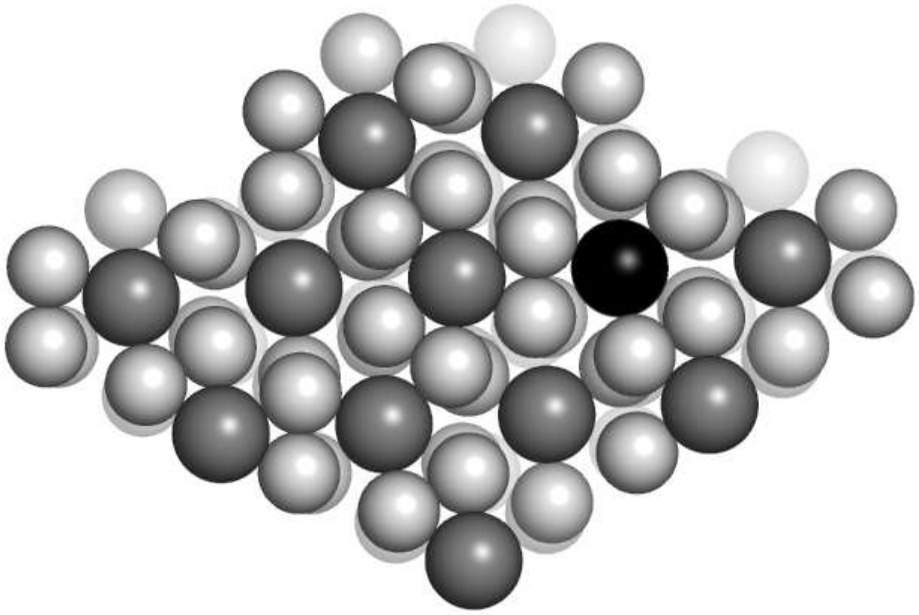

Figure 3.14: Relaxed structure of surface interacting with chlorine in vacuum: oxygen (light gray spheres), chromium (dark gray spheres), and chlorine (black sphere): top view ([0001] direction perpendicular to page).

the clean surface structure (movement of all surface atoms is less than 0.01 Å) with the chlorine ion settling upon relaxation to a position with a chlorine-oxygen separation of 2.6 Å, only 20% smaller than the sum of the nominal ionic radii, 3.1 Å. Figure 3.15a shows a side view of the total electron density for a surface with adsorbed Cl in vacuum, illustrating the physisorbed nature of the interaction.

Turning to the energy levels, Figure 3.3c.1 shows the levels near the gap. In this case, three two-thirds filled states (degenerate to within 19 meV$\sim$ 220 K) appear just below the top of the gap, indicating the presence of a hole in the Cr band, which we interpret as arising from the chlorine atom absorbing an electron from

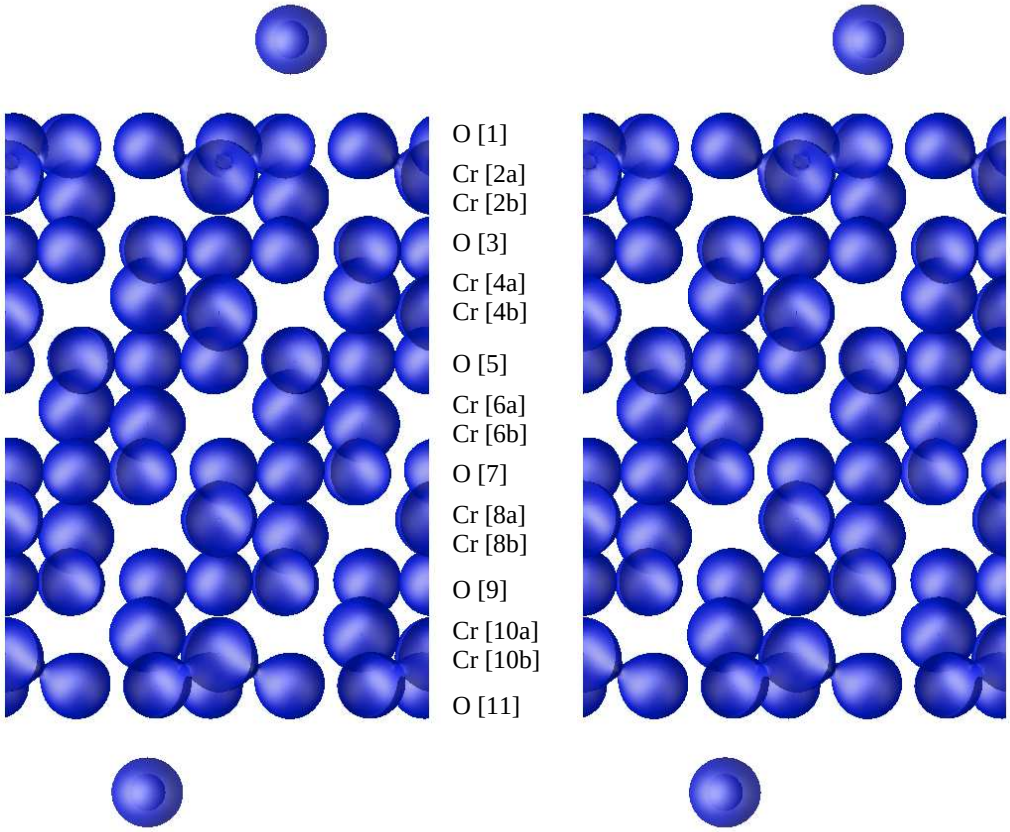

(a) (b)

Figure 3.15: Contour level ($0.68\ e^{-}/\text{Å}^3$) of total electron density for chlorine atom adsorbed on oxygen-terminated (0001) surface in (a) vacuum and (b) dielectric, side view ([0001] direction runs vertically up the page). Atomic layers indicated as in Figure 3.2. Note that densities are such that the contours appear spherical.

the chromium oxide to become Cl^-. To explore local effects from the adsorbed chlorine, Figure 3.16 presents the local density of states, weighing each state with the probability of an electron being within 1.6 Å of the chlorine nucleus. In contrast to the local density of states of the hydrogen calculation, the appearance of the oxygen band is significantly reduced and there is much stronger mixing with the bulk chromium states. This mixing corresponds to alignment of the barely bound Cl^- states with the bulk HOMO chromium band as the chlorine ion draws electrons from the bulk chromium band, which is serving as a reservoir of electrons. Finally, Figure 3.17a shows the sum of the electron probabilities in the partially filled states at the Fermi level, which are thus both the HOMOs and the LUMOs. Interpreted as the sum of states lacking exactly one electron from full occupancy, the figure shows the spatial distribution of the hole which the formation of the Cl^- injects into the chromium-oxide slab. As one would expect, this (positive) hole tends to localize to the vicinity of the Cl^- ions.

Upon relaxation of the physisorbed chlorine surface in the presence of the solvent, we find there to be very little relaxation (no more than 0.01 Å for any atom), little difference in the total charge density (Figure 3.15b), no change in the presence of partially filled states at the Fermi level (Figure 3.3c.2), and very little difference in the local density of states (Figure 3.16) or the spatial distribution of the hole injected into surface, Figure 3.17b.

3.5.4 Conclusions

Above, we give an application of the novel approach of using a joint density-functional theory to treat an *ab initio* electronic structure calculation in the presence of a liquid solvent such as water. Through this approach, we find the mode

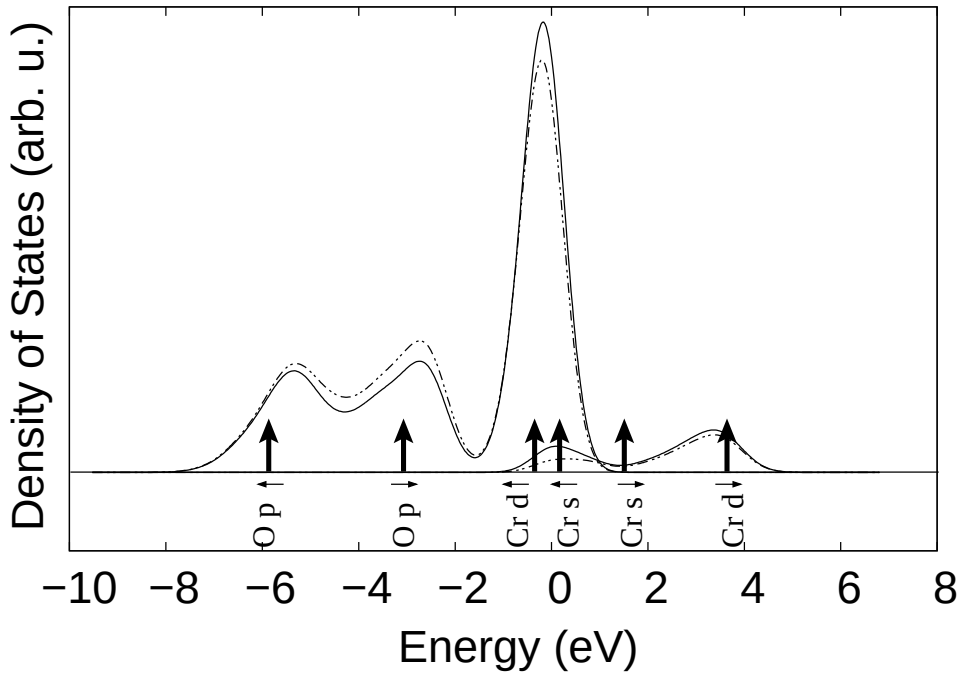

Figure 3.16: Local density of states within 1.6 Å of the chlorine nucleus for chlorine interacting with the oxygen-terminated (0001) surface in vacuum (solid curve) and solution (dashed curve). Same conventions as Figure 3.4.

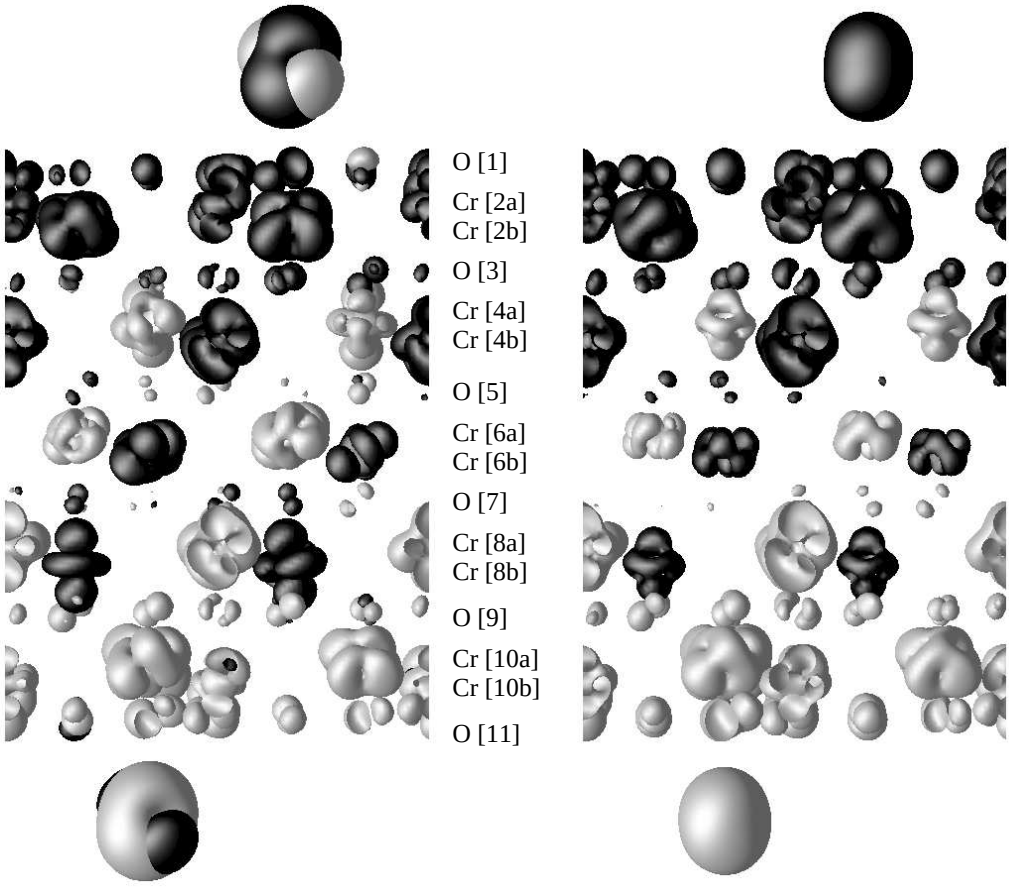

(a) (b)

Figure 3.17: Contour level ($0.68\, e^{-}/\text{Å}^3$) of HOMOs and LUMOs (equivalent in this case) of chlorine interaction with oxygen-terminated (0001) surface in (a) vacuum and (b) dielectric, side view ([0001] directions runs vertically up the page). Atomic layers indicated as in Figure 3.2.

of interaction of the oxygen-terminated Cr_2O_3 (0001) surface with hydrogen to be covalent bonding while that with chlorine to be ionic bonding. The presence of a dielectric solvent has very little effect on the pristine surface or on its interaction with chlorine, while it has a dramatic affect on the interaction with hydrogen. In vacuum, hydrogen readily forms an O-H bond with the outermost layer of atoms of the surface. In the presence of water, the strong screening associated with dielectric effects in the vicinity of the proton (ultimately via hydrogen bonding interactions) so weakens the attractive potential of the proton that the covalent bond is broken, the electron is released into the surface, and the proton solvates.

In contrast, the interaction with chlorine in vacuum is already ionic, with a neutral chlorine atom having sufficient electronegativity to draw an electron from the bulk of the crystal and thus ionize to Cl^- while injecting a hole into the bulk. The presence of a dielectric solvent tends to screen the excess charge on the chlorine ion, thereby only further stabilizing this form of interaction with the surface so that there is little change in this case when going from vacuum to a dielectric environment. It thus appears that the primary reason why the solvent has a much greater effect on the interaction with hydrogen than with chlorine is that a dielectric environment generally favors the formation of ions and the surface interaction with chlorine is already ionic whereas the interaction with hydrogen in vacuum is covalent.

We believe that there would be little effect on these conclusions were the calculations to be performed with ions rather than atoms. Doing so would involve principally removing a single electron from the calculation for each hydrogen atom or adding an electron for each chlorine atom. For the chlorine cases, this would simply remove the relatively delocalized hole from the bulk chromium band and

thus likely have little effect on the final results. For the interaction with hydrogen, the removal of an electron from our calculation as performed currently would, in the dielectric case, likely simply remove the relatively delocalized donated electron or, in the vacuum case, likely simply introduce a relatively delocalized hole into the chromium band. In either of these cases for hydrogen, we again would expect little change in the results of our calculations. To make a definitive statement for the precise behavior of a proton on the surface, future calculations should include the more detailed variational principle of Eq. (2.7) and at least a few water molecules so as to allow for the Grotthus mechanism (proton diffusion via bond switching events in the water environment). However, allowing the Grotthus mechanism would seem only to make departure of the proton into the solution more likely. Thus, although we cannot draw a definitive conclusion at this point, we feel that with protons, as we have found with hydrogen atoms, there will be little disruption of the chemical integrity of the surface.

Overall, a novel picture emerges to explain how the oxygen-terminated surface of Cr_2O_3 is particularly protective in a hydrochloric acid solution. The outer oxygen layer provides a natural barrier to interaction with chlorine but might be expected to interact strongly with protons. However, through dielectric screening effects, it is the aqueous environment itself which eliminates the outer oxygen layer's natural tendency to interact with hydrogen.

Our calculations of surface chemistry in the presence of a solvent make clear the need for additional work to complete the picture of the passivating effects of chromium oxide. We would next like to study the interaction of chlorine and hydrogen with a *chromium*-terminated surface, whose HOMOs would then be exposed on the surface rather than protected under the outer oxygen layer. We also would

like to explore pit corrosion by calculating the interaction of the aforementioned species with a step in the passivating oxygen layer. Finally, we would like to contrast the interactions of chlorine in such systems to the interactions of fluorine and bromine in order to better understand the corrosive success of chlorine relative to these other species.

Bibliography

[1] M. R. Radeke and E. A. Carter, Annual Review of Physical Chemistry **48**, 243 (1997).

[2] J. Greeley, J. K. Norskov, and M. Mavrikakis, Annual Review of Physical Chemistry **53**, 319 (2002).

[3] A. Gross, Surface Science **500**, 347 (2002/03/10).

[4] J. DeGaspari, Mechanical Engineering **125**, 30 (2003).

[5] M. P. Ryan *et al.*, Nature **415**, 770 (2002).

[6] C. Stampfl, M. V. Ganduglia-Pirovano, K. Reuter, and M. Scheffler, Surface Science **500**, 368 (2002).

[7] J. Erlebacher *et al.*, Nature **410**, 450 (2001/03/22).

[8] D. A. Jones, *Principles and Prevention of Corrosion* (Prentice Hall, Upper Saddle River NJ, 1996).

[9] R. Latanision *et al.*, in *Fourth International Symposium on Supercritical Fluids* (Sendai, Japan, 1997), Vol. C, pp. 865 – 868.

[10] S. Alavi, D. C. Sorescu, and D. L. Thompson, Journal of Physical Chemistry B **107**, 186 (2003).

[11] J. A. Cline, A. A. Rigos, and T. A. Arias, Journal of Physical Chemistry B **104**, 6195 (2000).

[12] D. Tannor *et al.*, Journal of the American Chemical Society **116**, 11875 (1994).

[13] J.-L. Fattebert and F. Gygi, Journal of Computational Chemistry **23**, 662 (2002).

[14] D. Henderson, *Fundamentals of Inhomogeneous Fluids* (Marcel Dekker, New York, 1992).

[15] S. Sun, Physical Review E (Statistical, Nonlinear, and Soft Matter Physics) **64**, 021512 (2001).

[16] J. Perdew and Y. Wang, Physical Review B (Condensed Matter) **45**, 13244 (1992/06/15).

[17] M. Payne *et al.*, Reviews of Modern Physics **64**, 1045 (1992).

[18] L. Kleinman and D. Bylander, Physical Review Letters **48**, 1425 (1982).

[19] T. Arias, M. Payne, and J. Joannopoulos, Physical Review Letters **69**, 1077 (1992/08/17).

[20] J. Tomasi and M. Persico, Chemical Reviews **94**, 2027 (1994).

[21] B. Marten *et al.*, Journal of Physical Chemistry **100**, 11775 (1996).

Chapter 4

Classical Density-Functional Theory for Water

Chapter 3 introduced the local dielectric approximation for water, which accounted only for the electrostatic interactions in a very approximate way but completely neglected cavitation energies. This chapter explores the development of classical density-functional theories for water to allow description of such cavitation energies. We explore how the best known approximate form for the classical density functional, the weighted density approximation, fails when applied directly to water. We then introduce a new, computationally efficient and accurate classical density-functional theory for water and apply it to the hydration of hard spheres and inert gas atoms. We find relatively good agreement with molecular dynamics simulations for the hydration of small hard spheres of radii relevant to molecules in solution, and we find rough agreement for the solvation of inert gas atoms in water. Our attempts to describe inert gas atoms, however, clearly point to the need to explore orientationally dependent density functionals for liquid water.

4.1 Introduction

Despite its importance to a wide range of problems in chemistry and biology, relatively little progress has been made in the first principles understanding of the microscopic structure of water and its interaction with solutes. The underlying reason for this is that, in the liquid state, the kinetic energy of molecules is on the same order as their interaction energy, so that the perturbative methods which

have proved so successful for solids and non-ideal gases fail.

For the study of liquids and their interactions with external systems, two general classes of theoretical methods have been developed. The first treats the liquid as a collection of molecules treated either *ab initio* within density-functional theory or with a model interatomic potential, such as the simple point charge (SPC) model [1] or the 4-site transferable intermolecular potential TIP4P [2], and then uses molecular dynamics (MD) or Monte Carlo numerical methods to perform statistical averaging over the thermal phase space[3, 4, 5]. These methods are intuitively simple to understand and also relatively straightforward to implement numerically. However, because they involve statistical averaging of many molecules over an exponentially growing configuration phase space, these methods are numerically very demanding. The second class of methods treats the liquid as a continuous media[6, 7, 8, 9, 10]. Without the need for thermal averaging or to represent molecules individually, these latter methods are much more efficient computationally. However, such models are generally built in an empirical way and, generally, there is no systematic way to improve them. Nonetheless, significant progress has been made in understanding the interaction of water with external environments using this approach, such as the work of Pratt and Chandler [11] on the theory of the hydrophobic effect and the Lum, Chandler, Weeks (LCW) theory of hydrophobicity[12].

In this chapter, we explore the nature of the interaction of water with external environments using a somewhat different approach than that of Chandler and coworkers and work in the classical density-functional theory framework reviewed briefly in Section 1.2 of this thesis. There are two main advantages of working in this framework. First, the classical density-functional theory of liquids is a continu-

ous theory of the liquid state which is exact in principle. Moreover, this framework gives the free energy and the density profile of the liquid in *any* external potential $V(\vec{r})$ in terms of a single density-functional[13], so that study of the hydrophobic effect (liquid in contact with either an impenetrable wall or an impenetrable hard sphere) and of the interaction of the liquid with any solute can be carried out in a single, unified framework. A number of approximate density-functionals have been developed for water and applied to the hydrophobic effect[9, 14]. Much more demanding theories which go beyond the average molecular density to consider explicitly the distribution of molecular orientations in water have also been developed[15, 16]. These current density functional theories, however, prove to be either quite computationally demanding or to provide an over-simplified description.

We begin this work by introducing a computationally efficient density-functional theory for water which reproduces the hydrophobic effect near hard boundaries. We then present the first application of a classical density-functional theory to realistic *ab initio* potential energy surfaces of solutes, applying our theory to the solvation of the inert gas sequence. This latter study allows us to address directly the question of whether explicit orientation dependence, with all of the concomitant computational demands, is necessary to provide an accurate description of the solvation of even the simplest solutes.

4.2 Failure of traditional weighted-density functional form

Our density-functional theory is inspired by the class of weighted-density functionals [17, 18] described in Section 1.2. We begin with a simpler, non-self-consistent

form of the weighted density approximation due to[18],

$$F_{ex}[\rho(\vec{\mathrm{r}})] = \int d\vec{\mathrm{r}}\rho(\vec{\mathrm{r}}) f_{ex}(\bar{\rho}(\vec{\mathrm{r}}))$$

where $f_{ex}(\bar{\rho}(\vec{\mathrm{r}}))$ is the excess free energy per particle of the inhomogeneous liquid at $\vec{\mathrm{r}}$ and

$$\bar{\rho}(\vec{\mathrm{r}}) = \int d\vec{\mathrm{r}}' w(\vec{\mathrm{r}} - \vec{\mathrm{r}}'; \rho_0)\rho(\vec{\mathrm{r}}').$$

This theory gives the direct correlation function

$$c(\vec{\mathrm{r}_1} - \vec{\mathrm{r}_2}; \rho_0) = -\beta \frac{\delta^2 F_{ex}[\rho]}{\delta\rho(\vec{\mathrm{r}_1})\delta\rho(\vec{\mathrm{r}_2})},$$

in Fourier space as

$$c(k;\rho_0) = -\beta\rho_0 \frac{\partial^2 f_{ex}}{\partial\rho^2} w^2(k;\rho_0) - 2\beta \frac{\partial f_{ex}}{\partial\rho} w(k;\rho_0), \tag{4.1}$$

which may be solved for the unknown function $w(k)$ given experimentally derived data for $c(k)$.

Experiments generally give results from which the oxygen total correlation function $h(r) \equiv g(r) - 1$ may be extracted. Figure 4.1 presents results from [19] along with a fit to an analytic function which we used for our numerical calculations,

$$\begin{aligned} h(k) = \; & - \; 4\pi r_a \frac{\mathrm{sinc}(kr_a) - \cos(kr_a)}{k^2} e^{-k^2/2\sigma_a^2} \\ & + \; A r_b \mathrm{sinc}(kr_b) e^{-k^2/2\sigma_b^2} + B r_c \mathrm{sinc}(kr_c) e^{-k^2/2\sigma_c^2}, \end{aligned} \tag{4.2}$$

where the values of the various parameters appear in Table 4.2. From the total correlation function $h(k)$, the direct correlation function $c(k)$ may be obtained directly in Fourier space from the Ornstein-Zernike equation,

$$1 + \rho_0 h(k) = \frac{1}{1 - \rho_0 c(k)}.$$

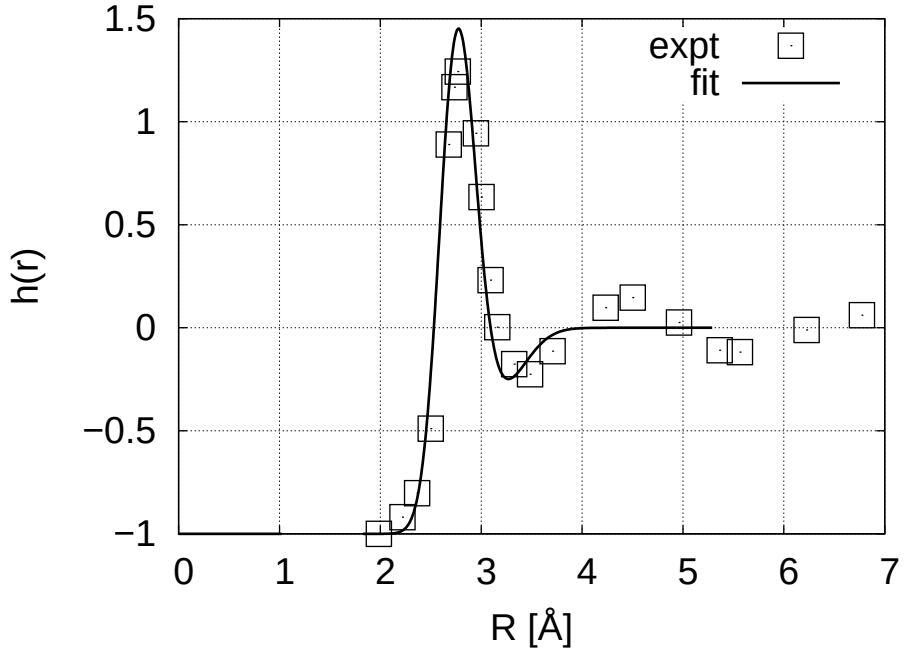

Figure 4.1: Oxygen-oxygen total correlation function in liquid water: experimentally determined data of [19] (squares), Fourier transform of fitted analytic function Eq. (4.2) (curve)

Table 4.1: Fitted values of parameters in Eq. (4.2)

A=90 B^2	B=-28.75 B^2	
r_a=4.89 B	r_b=5.25 B	r_c=6.0 B
σ_a=4 B	σ_b=3 B	σ_c=2 B

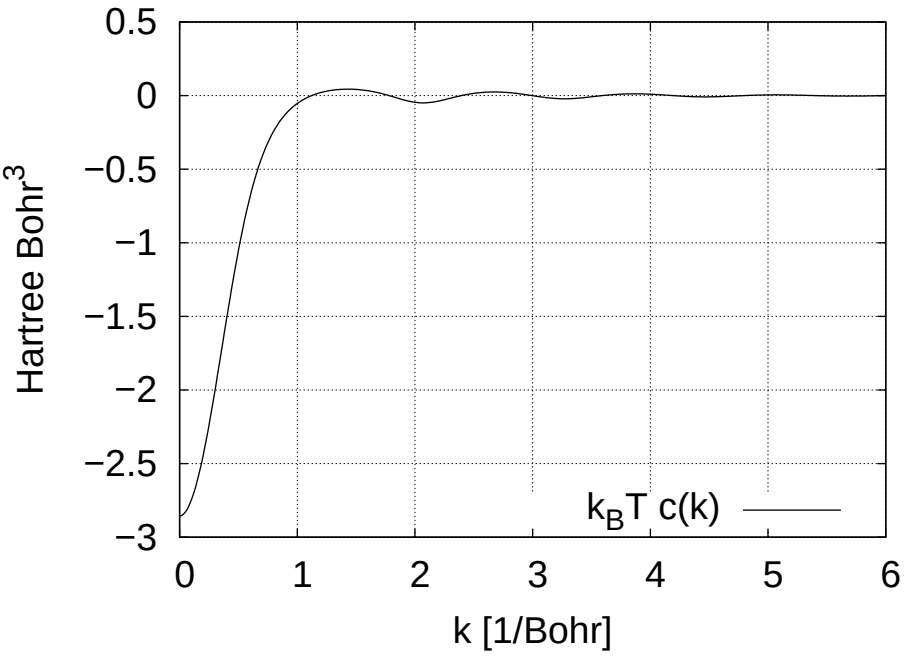

Figure 4.2: Direct oxygen-oxygen correlation function for liquid water in Fourier space extracted from experimental data

Finally, Figure 4.2 presents our results for $c(k)$.

For liquids with attractive interactions in general and for water in particular, these equations are known not to allow appropriate solutions [9, 6]. As a quadratic equation, Eq. (4.1) has two roots for $w(k)$. Figure 4.3 shows the real part of the solution of Eq. (4.1) for water under standard conditions. The flat regions of the result correspond to points where the solution has become complex. Isotropy requires that $w(\vec{r}-\vec{r}')$ be spherically symmetric so that $w(k)$ must be real. Thus, although Eq. (4.1) gives the appropriate condition for the functional to reproduce the pair correlation functions, there is no choice for $w(\vec{r}-\vec{r}')$ which will reproduce correlations in the fluid. Sun[9] also reports inability to solve the equation for $w(k)$ for certain values of k, even for the self-consistent weighted density functional theory.

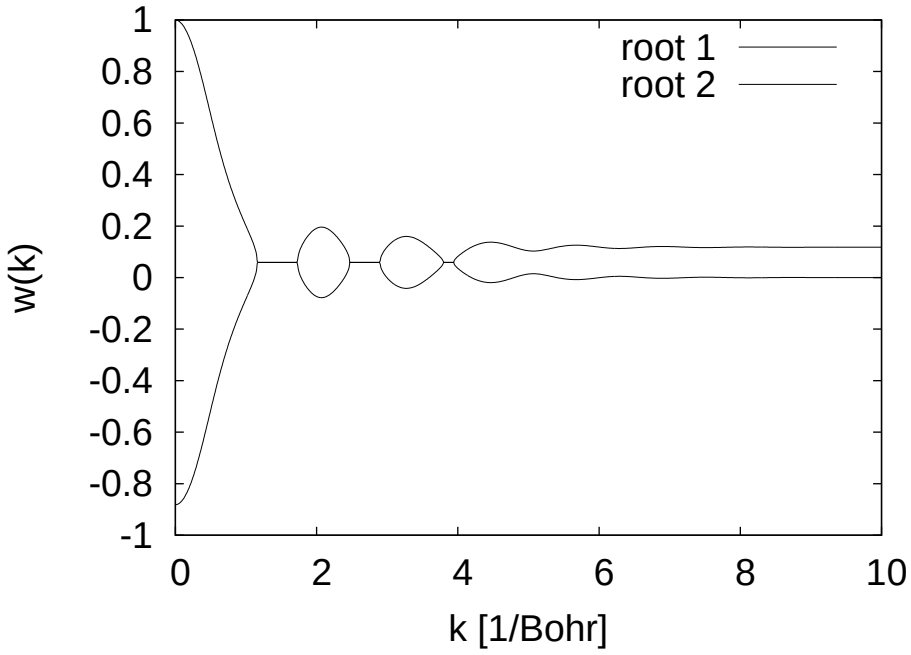

Figure 4.3: Two roots of Eq. (4.1) for $w(k)$ (real part)

From Figure 4.3 it might appear that the failure to find an appropriate $w(k)$ to reproduce $c(k)$ comes from a peculiarity in $c(k)$ rather from the structure of the equations. It also appears that a relatively small change to $c(k)$ would yield real solutions. This suggests the following alternative functional,

$$F_{ex}[\rho(\vec{\mathrm{r}})] = \int d\vec{\mathrm{r}}\rho(\vec{\mathrm{r}}) f_{ex}(\bar{\rho}(\vec{\mathrm{r}})) + \frac{1}{2}\iint d\vec{\mathrm{r}}d\vec{\mathrm{r}}'\rho(\vec{r})\chi(\vec{r}-\vec{r}')\rho(\vec{r}'), \tag{4.3}$$

in which most of the physics can still be captured in the $f_{ex}(\bar{\rho})$ term, with relatively small corrections provided by the quadratic kernel χ to maintain exact recovery of the two-point correlation function. From (4.3), we then have

$$c(k) + \beta\chi(k) = -\beta\rho_0 \frac{\partial^2 f_{ex}}{\partial\rho^2} w^2(k;\rho_0) - 2\beta\frac{\partial f_{ex}}{\partial\rho} w(k;\rho_0) \tag{4.4}$$

so that the new left-hand side may be made to take on values such that real solutions exist. However, although this equation can be arranged to always yield real solutions, each branch of that solution will always violate one of the basic

limiting conditions on $w(k)$, either that $w(k=0)=1$ so that the free energy of the uniform liquid is reproduced or that $w(k\to\infty)=0$ so that $w(\vec{r}-\vec{r}')$ contains no delta function, allowing the ideal gas part $F_{id}[\rho]$ to capture properly all high frequency behavior. Specifically, one may show as a property of the quadratic formula that, because for water it happens that $\partial f_{ex}(\rho)/\partial\rho < 0$, the branch of the solution which approaches unity as k approaches zero is not the same branch which approaches zero as k approaches infinity. The additional function $\chi(k)$ cannot change this because physically reasonable $\chi(k)$ must approach zero in both of these limits: so as not to disturb the free energy of the uniform liquid, $\chi(\vec{r})$ must integrate to zero, so as to properly capture high spatial frequency behavior with $F_{id}[\rho]$, $\chi(k)$ must vanish as $k\to\infty$.

This difficulty can be removed by considering higher order correlations [20]. However, such correlations increase the computational complexity significantly and the required experimental information may not be available. This thesis explores the alternative route of staying with two particle correlations but exploring new functional forms.

An intriguing modification which always yields real solutions for $w(k)$ without the device of introducing χ is to write

$$F[\rho(\vec{r})] = F_{id}[\bar{\rho}(\vec{r})] + \int d\vec{\mathrm{r}} f_{ex}(\bar{\rho}(\vec{\mathrm{r}})).$$

In this case, the direct correlation function obeys

$$1-\rho_0 c(k) = \beta\rho_0 \left.\frac{\partial^2(F_{id}(\rho)+f_{ex}(\rho))}{\partial\rho^2}\right|_{\rho=\rho_0} |w(k)|^2 .$$

Now, because the Ornstein-Zernike equation ensures $1-\rho_0 c(k) = \frac{1}{S(k)} > 0$, real solutions for $w(k)$ will always exist. Unfortunately, because $S(k\to\infty)\to 1$, $w(k)$ is finite as $k\to\infty$, which, again, ultimately produces invalid results for quantities

in the high frequency limit, such as the hydration energy of small spheres $R \to 0$.

4.3 Construction of classical density-functional theory for water

This section builds on the preceding experience to construct a successful classical density functional theory for water. The final method is computationally much simpler that the full weighted density-functional approach in that it does not require computationally demanding self-consistent calculations of the weighted density. On the other hand, our form does allow us to incorporate much of the same physics as [6] and to thus find a form which is competitive computationally but more accurate than other, more simplified functionals[9].

The primary differences between our form and the traditional form are to introduce the quadratic kernel from the first attempted functional above and, from the second failed functional above, to not separate the excess free energy per unit volume into a product of the local density and an excess free energy per particle. In particular, we write

$$\begin{aligned} F[\rho(\vec{r})] &= F_{id}[\rho(\vec{r})] + \int f_{ex}(\bar{\rho}(\vec{r}))d\vec{r} \\ &\quad + \frac{1}{2}\iint \rho(\vec{r})\chi(\vec{r}-\vec{r}')\rho(\vec{r}')d\vec{r}d\vec{r}', \end{aligned} \tag{4.5}$$

using the local density in $F_{id}[\rho(\vec{r})]$ ensures exact treatment of short length-scale properties through the first term in Eq. (4.5), which is known exactly. Again, so that the new, final term does not affect the free energy of the uniform fluid, we choose to consider only $\chi(\vec{r})$ which integrate to zero and so that the high-frequency behaviors from the ideal gas component are not affected, we insist also that $\chi(k \to \infty) \to 0$.

Within this theory, the direct correlation function obeys

$$c(k) + \beta\chi(k) = \beta \left. \frac{\partial^2 f_{ex}(\rho)}{\partial \rho^2} \right|_{\rho=\rho_0} |w(k)|^2 .$$

Figure 4.4 shows $k_B T c(k)$ and the resulting $\chi(k)$ when choosing $w(k)$ as normalized Gaussian so that

$$\bar{\rho}(\vec{r}) \equiv (2\lambda^2\pi)^{-\frac{3}{2}} \int \rho(\vec{r}') e^{\frac{-|\vec{r}-\vec{r}'|^2}{2\lambda^2}} d\vec{r}', \tag{4.6}$$

where the width λ is chosen to best fit the resulting planar *surface tension* (Gibbs free energy per unit area[13]). ($\lambda = 0.4605$ a.u. reproduces the surface tension of bulk water 70 mN/m or 4.5×10^{-5} a.u.) Note that the resulting $\chi(k)$ is relatively small, so that most of the description of the physics remains in the non-linear $f_{ex}(\bar{\rho}(\vec{r}))$ part, with relatively small corrections in $\chi(k)$ to ensure exact description of the direct two-particle correlation function. As with the traditional weighted density-functional approximation, the non-linearity of the second term in Eq. (4.5) ensures that a large-scale phase separation between vapor and liquid is treated correctly.

To construct the functions and parameters needed in Eq. (4.5), we begin by noting that, for the uniform liquid, the last term gives zero (χ has zero integral) and $\bar{\rho}(\vec{r}) = \rho(\vec{r})$, so that $f_{ex}(\rho)$ can be constructed to reproduce the properties of the uniform liquid exactly. In practice, we parameterized $f_{ex}(\rho)$ as a sixth-order polynomial

$$f_{ex}(\rho) = a\rho^6 + b\rho^5 + c\rho^4 + d\rho^3 + e\rho^2 + f\rho + g. \tag{4.7}$$

with parameters chosen to reproduce, for bulk water at standard ambient temperature and pressure (SATP), the density and bulk modulus of both the liquid and vapor (four parameters), the derivative of the bulk modulus of the liquid with respect to pressure $\partial B/\partial P$ (one parameter), and phase coexistence of the

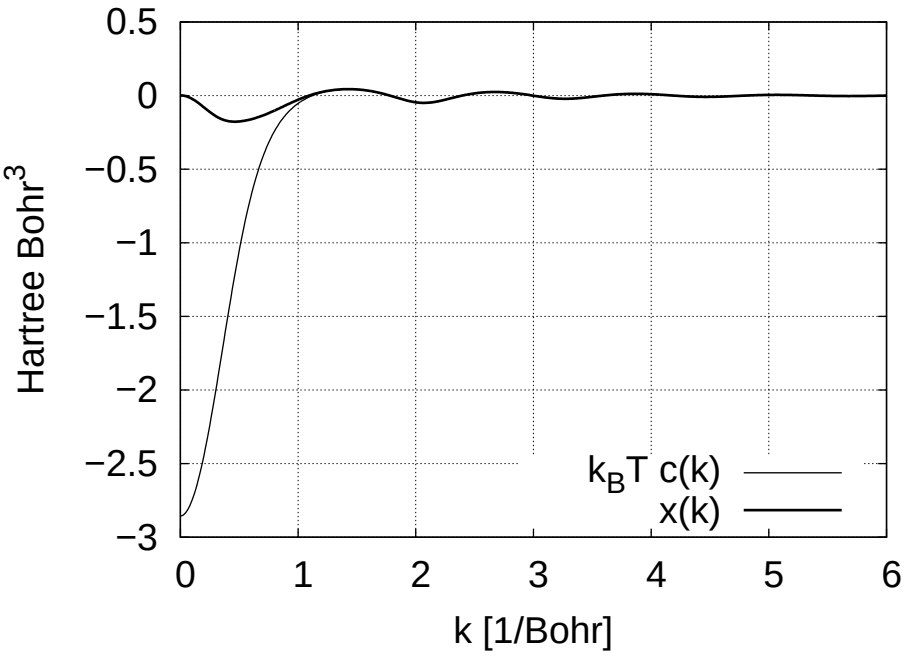

Figure 4.4: Direct correlation function $k_BTc(k)$ from Figure 4.2 and the residual $\chi(k)$.

liquid and vapor at the zero of free energy (two parameters). Table 4.2 gives both the fit data and the resulting parameters, and Figure 4.5 presents the final function $F(\rho)$. Note that in this work we employ mostly atomic units (a.u.) so that Planck's constant, the electron mass and the fundamental charge all have numerical value unity ($\hbar = m_e = e = 1$), implying that energies are measured in units of 1 hartree=27.21 eV and distances in units of 1 bohr=0.5291 Å. Finally, we emphasize that in constructing this functional we used only either uniform or macroscopic properties of water and have fit nothing to free energies of solution for any kind of solute.

Table 4.2: Properties of uniform bulk water at Standard Ambient Temperature and Pressure (SATP: T=25 °C, P=100.00 kPa)

Vapor density	0.023 kg/m^3	a	6.630×10^9	e	8.906×10^{-4}
Water density	997.1 kg/m^3	b	-1.277×10^8	f	-1.415×10^{-2}
Bulk modulus	2.187 GPa	c	9.200×10^5	g	1.077×10^{-10}
$\partial B/\partial P$	5.83	d	-2.602×10^3		

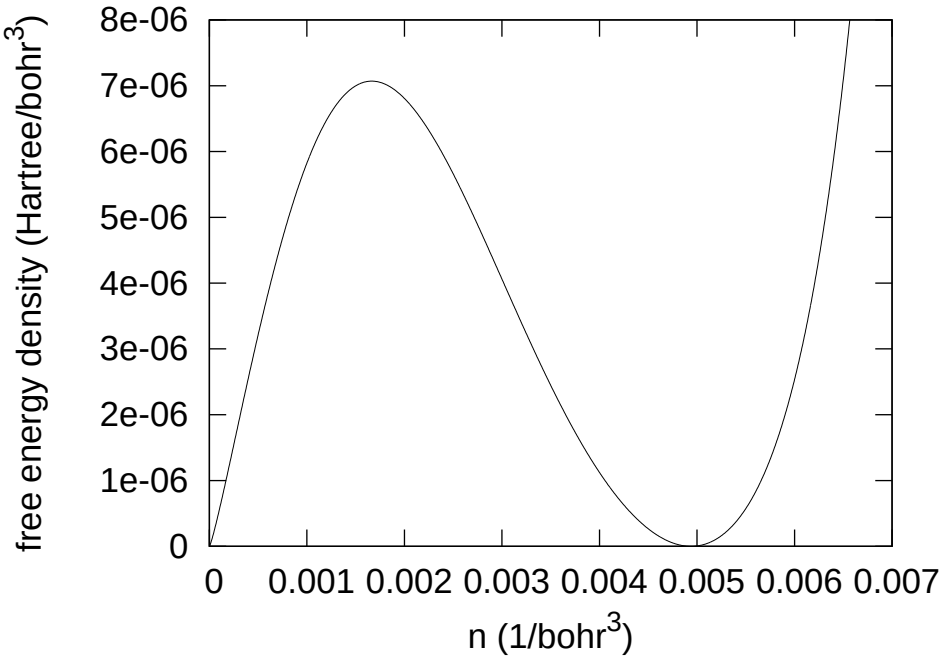

Figure 4.5: Free energy density of water as a function of its density at SATP

4.4 Application to hydration of hard spheres

To test the accuracy of this approximation we use it to calculate the free energy of a spherical cavity in water, a standard test case used in the literature [12, 9, 21, 22] to explore density variations in water over all possible length scales. The interaction potential with a hard sphere of radius R, defined so that the center of no molecule approaches within a distance R of the sphere center, is idealized because it depends only on the distance of the water molecule to the hard sphere and does not depend on the orientation. For instance, for a real water molecule it is unclear even what point to take to represent the location of the molecule. The position of the oxygen nucleus is most commonly taken.

Figure 4.6 compares our results for the surface tension (free energy change per unit area) of a spherical cavity with results of molecular simulations for SPC/E water[23]. The figure verifies that the surface tension approaches in the macroscopic value in the limit of large radii and shows that for smaller radii, the surface tension has a strong dependence on radius. Our results are in much better agreement with the molecular dynamics data than those of the original Lum-Chandler-Weeks[12] theory. The good agreement with explicit molecular dynamics simulations (very good for the small radii typical of solvated molecules and within 20% at the worst case) suggests that this model can be used to give a good quantitative description of the hydrophobic effect, a central problem of theoretical chemistry.

4.5 Application to hydration of inert gas atoms

The ultimate motivation for inhomogeneous continuous theories of bulk water is to understand solvation of real solutes, not artificial hard boundaries. Within

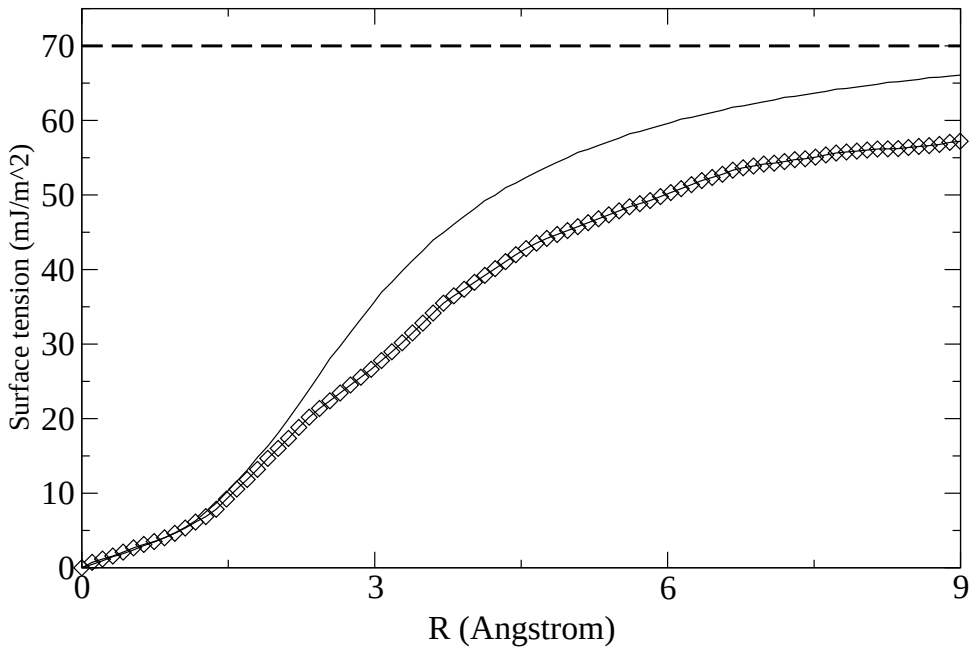

Figure 4.6: Surface tension of a hard sphere of radius R in water at SATP. Solid line denotes the results of our classical density-functional theory calculations. Molecular simulation results for a cavity in SPC/E water are indicated by diamonds [23]. Dashed line corresponds to macroscopic surface tension of water. R is defined as the distance of closest approach between molecular centers and sphere center.

the density-functional framework of Eq. (1.21), one can simply and rigorously incorporate the effects of any external potential $V(\vec{r})$ acting on the liquid, making treatment of real solutes simple in principle, provided a static potential $V(\vec{r})$ accurately describes the interaction of water with the solute. For our next test, we treat a simple but challenging problem for which there is experimental data, the solvation of inert gas atoms.

The experimental solubilities of the inert gasses in water give the corresponding solvation free energies directly. In the dilute limit, the free energy of solvation $\Delta\Omega$ relates to the mole fraction solubility through the relation

$$\Delta\Omega = k_B T \log\left(\frac{n_{\text{gas}}}{X_1 n_w}\right) = k_B T \log\left(\frac{1\text{atm}}{k_B T X_1 n_w}\right) \tag{4.8}$$

where X_1 is the mole fraction solubility in water and n_w is the number density of liquid water.

The experimental data, which Table 4.3 summarizes, show an interesting trend. Although the solvation energies of hard spheres increase with size, the solvation energies of inert gas atoms tend to *decrease*. (Note that for helium, the worst possible case, we estimate quantum zero-point effects to be quite small, on the order of 0.005 eV, so that this must be purely an effect of the interactions.) Thus, a simple cavity model for solvation of inert gas atoms is not a good approximation and one must use a more realistic interaction potential $V(\vec{r})$.

We determined the potential energy of interaction between a water molecule and an atom of each of the inert gasses in Table 4.3 directly through *ab initio* density-functional theory calculations within the generalized gradient approximation (GGA) [24]. For these calculations we take $\vec{r}$ to be the displacement between the nucleus of the inert gas and the nucleus of the oxygen atom and considered one hundred different orientations for the water molecule, with these orientations

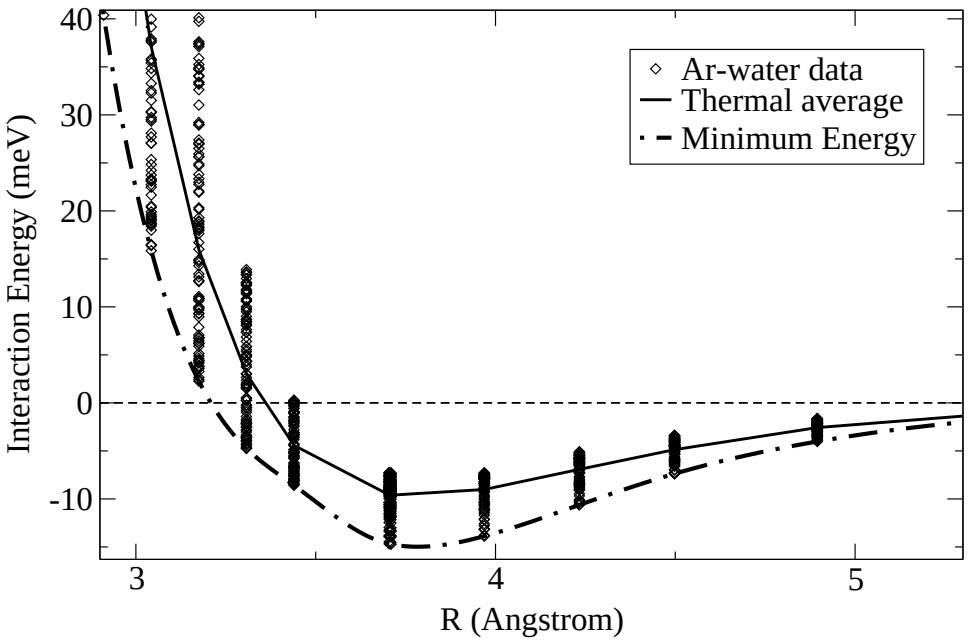

Figure 4.7: Interaction of Argon and a water molecule. Each diamond corresponds to a specific orientation. Also presented are the Boltzmann average potential (solid line) and the minimum potential (dot-dashed line).

optimized to sample the angular dependence evenly according to the procedure of Womersley and Sloan[25]. Figure 4.7 summarizes the results for argon, which was typical of all of the inert gasses considered in this work.

The scatter in the interaction energy at each distance r shows a strong dependence on the orientation of the water molecule, particularly at shorter distances. The question then immediately arises of how to couple to any continuum theory based solely on the molecular density $N(r)$ with no information about the orientation of the molecules in the solute. As the coupling in such *density-only* functional theories takes the form $\int V(\vec{r})n(\vec{r})d\vec{r}$, a choice must be made to define a unique value for the potential $V(\vec{r})$ for each point $\vec{r}$. One approach would be to assume, unrealistically, that each water molecule independently assumes its most favored

orientation for a given distance, thereby defining $V(r)$ as the minimum energy envelop ($V_{min}(r)$) of the data in Figure 4.7. Another approach would be to take the thermal average interaction under the, also unrealistic, assumption that the water molecules choose their orientations independently of each other, thereby defining $V(r)$ as the Boltzmann weighted average ($V_{kT}(r)$) of the data at each distance. The fact that there is no satisfactory answer for a definitive choice for $V(\vec{r})$ underscores the need in future work to include some sort of orientational information into the density functional description of water. For now, we explore the accuracy that can be obtained with non-orientation dependent functionals in conjunction with the above two choices, V_{min} and V_{kT}.

Table 4.3 summarizes the results of the minimum free energy of our functional for both of the above choices for the external potential. As expected, the use of the minimum envelop V_{min} provides a lower bound on the experimental solvation energies. This choice, for the larger atoms Ar and Kr, also reproduces the experimental trend of lower solvation energies for larger atoms, confirming that there is sufficient attraction in the negative portions of the interaction (as evident in Figure (4.7) to more than compensate increased size of the cavity.

Alternately, using the Boltzmann averaged potential V_{kT} does provide more accurate results in the sense that the maximum error is 0.1 eV, although the trend in decreasing energy with increasing size is not well reproduced. Evidently, the "true" potential, if such exists, lies between these extremes. Although 0.1 eV is on the order of the interactions explored here, this is actually a promising result because the accuracy of typical electron density functional theories, such as the local density approximation, is also on this order. Thus, the accuracy of this theory in capturing the hydrophobic effect should be sufficient for most applications of a

Table 4.3: Solvation energies of inert gas atoms

	Exp. (eV)	V_{kT} (eV)	V_{min} (eV)
Helium	0.12	0.12	0.07
Neon	0.12	0.05	−0.02
Argon	0.09	0.19	0.09
Krypton	0.07	0.19	0.08

joint-density functional theory. The errors only appear to be large in this context because of the challenging nature of describing the subtle interactions between water and noble gas atoms. For more typical molecules with stronger electric fields, the hydrophobic effect is a relatively small correction to the total solvation energy and, although more work is clearly needed, the present approach should give at least workable results.

4.6 Conclusions and future directions

This chapter presents a simple density-functional theory for water which gives good agreement with molecular dynamics simulation data for the solvation of hard spheres in water. We find that even for non-polar solutes the orientation of water molecules plays an important role in solvation. Thus, although solvation of hard spheres is well described by density-only theories, such a theory does not necessarily adequately describe the solvation of even simple solutes such as inert gases. While we obtain promising results indicating that some form of density-functional theory can explain the counter-intuitive trend of decreasing energy with increasing size in the inert gas sequence, it appears that, particularly for non-polar solutes, treatment of orientation in some form is needed to attain results approaching so-

called “chemical accuracy,” accuracy sufficient to predict accurately reaction rates at standard conditions of room temperature, 0.025 eV. Nonetheless, the functional presented here should be sufficient for use in joint density functional theories employing standard approximations for the electron density functional whose uncertainties are comparable to those of the functional presented here, ~ 0.1 eV.

Bibliography

[1] H. J. C. Berendsen, J. P. M. Postma, W. F. van Gunsteren, and J. Hermans, *Intermolecular Forces* (Reidel, Dordrecht, 1981), p. 331.

[2] W. Jorgensen *et al.*, J. Chem. Phys. **79**, 926 (1983).

[3] P. Kollman, Chem. Rev. **93**, 2395 (1993).

[4] G. M. Torrie and J. Valleau, J. Comput. Phys. **23**, 187 (1977).

[5] E. A. Carter, G. Ciccotti, J. T. Hynes, and R. Kapral, Chem. Phys. Lett. **156**, 472 (1989).

[6] W. Curtin and N. W. Ashcroft, Phys. Rev. A **32**, 2909 (1985).

[7] J. Tomasi and M. Persico, Chem. Rev. **94**, 2027 (1994).

[8] B. Roux and T. Simonson, Bioph. Chem. **78**, 1 (1999).

[9] S. X. Sun, Phys. Rev. E **64**, 021512 (2001).

[10] J. D. Thompson, C. J. Cramer, and D. G. Truhlar, J. Chem. Phys. **119**, 1661 (2003).

[11] L. Pratt and D. Chandler, J. Chem. Phys. **67**, 3683 (1977).

[12] K. Lum, D. Chandler, and J. D. Weeks, J. Phys. Chem. **103**, 4570 (1999).

[13] J.-P. Hansen and I. McDonald, *Theory of Simple Liquids* (Elsevier, USA, 2006).

[14] T. F. Meister and D. M. Kroll, Phys. Rev. A **31**, 4055 (1985).

[15] R. Ramirez and D. Borgis, J. Phys. Chem. **109**, 6754 (2005).

[16] K. Ding, D. Chandler, S. J. Smithline, and A. D. J. Haymet, Phys. Rev. Let. **59**, 1698 (1987).

[17] S. Nordholm, M. Johnson, and B. Freasier, Australian Journal of Chemistry **33**, 2139 (1980).

[18] P. Tarazona, Molecular physics **52**, 81 (1984).

[19] A. K. Soper, F. Bruni, and M. A. Ricci, J. Chem. Phys. **106**, 247 (1997).

[20] C. N. Likos and N. W. Ashcroft, J. Chem. Phys. **99**, 9090 (1993).

[21] D. M. Huang, P. L. Geissler, and D. Chandler, J. Phys. Chem. B **105**, 6704 (2001).

[22] G. Hummer *et al.*, Proc. Natl. Acad. Sci. USA **93**, 8951 (1996).

[23] P. R. ten Wolde, S. X. Sun, and D. Chandler, Phys. Rev. A **137**, 1441 (1965).

[24] J. P. Perdew, K. Burke, and M. Ernzerhov, Phys. Rev. Lett. **78**, 3865 (1997).

[25] R. S. Womersley and I. H. Sloan, Adv. in Comp. Math. **114**, 195 (2001).

Chapter 5

Joint Density-Functional Theory for Electronic Structure of Solvated Systems

The preceding chapters introduced a theorem that allows joint treatment of electronic and classical density functionals, advanced the state-of-the-art of classical density-functional descriptions of water, and introduced a simple local dielectric model for coupling the electrons of the solute to the solvent. This final chapter combines all of these ideas, introducing a new model density functional for the *ab initio* description of electronic systems in contact with a molecular liquid environment. The resulting density-functional theory joins an electron density-functional for the electrons of a solute with a classical density-functional theory for the liquid into a single variational principle for the free energy of the combined system. A simple, approximate model functional predicts solvation energies, without any fitting of parameters to solvation data, at least as well as state-of-the-art quantum-chemical cavity approaches, which require such fitting. While more work is needed in the future to capture more of the underlying physics correctly, the results obtained with the current simplified model are encouraging and suggest that even better accuracy might be obtained when more of the physics is described correctly.

5.1 Introduction

Ab initio electron density-functional methods have proved a computationally efficient and accurate tool for the exploration of a wide range of issues in condensed-matter physics and chemistry. (See, for instance [1, 2].) However, application of

this approach is largely limited to the solid-state, gas phase chemistry, or to surface chemistry in high vacuum environments, with practical problems involving liquid environments largely out of reach. The reason for this unfortunate limitation is that proper description of the effects of water demands not only the inclusion of many solvent molecules but also thermodynamic sampling of many configurations of those molecules so as to properly capture the structure and response of the liquid over experimental length and time scales. Thus, the applicability of such approaches to the vast array of problems involving liquid environments, from liquid fuel-cell research to biochemistry, is severely curtailed.

In response, much effort (many thousands of articles and a large number of reviews, [3, 4, 5, 6, 7] and others, in the last decade alone) has been dedicated to the development and application of a large number of different "continuum" solvation models, in which the details of the molecular aqueous environment are replaced by a continuum description. More recently, Dzubiella et al.[8] developed a continuum model for water where hydrophobic, dispersion and electrostatic energy terms are written as functionals of the exclusion volume. The plethora of models evidences the importance of the problem, but the lack of a consensus underscores that no truly satisfactory method has been found.

The weaknesses of the current state of the art in continuum solvation approaches arises from their basic structure. As Ref. [7] and the other reviews cited above describe, such approaches generally divide the free energy of solvation into a number of contributions, typically cavitation (formation of the solvent-solute interface), dispersion (long-range electron correlations), repulsion (short-range electron overlap effects), and electrostatic (reorientational and polarization screening in the solvent). Work then proceeds to develop models for each of these terms separately.

The models for these terms generally require a cavity shape, which is most usually defined by spheres representing atoms or functional groups, where the sphere radii are determined by fits of the final results to a large *empirical* database of solvation energies[3]. Finally, to account for nonlinear saturation effects near solutes, an intermediate dielectric constant is often used in a shell around the solute as a buffer between the solute and bulk medium, as in Ref. [9] for example. Despite the successes of this method, the *ad hoc* separation of physical effects (all originating ultimately from the underlying quantum and statistical mechanics) and the empirical fitting to precisely the class of quantities of interest limits the reliability of the predictions of these models. This is especially true for applications to new classes of chemical species or to situations outside of the fitting database, such as to study liquid phase surface catalysis.

The new approach which we propose to pursue here relieves many of the aforementioned difficulties. As shown below, even a preliminary implementation of this new approach gives results which are competitive with state-of-the-art continuum solvation models, even without fitting to any solvation data whatsoever, suggesting that further refinements which incorporate more of the physics beyond what we manage to accomplish here has the promise to produce a new, efficient and predictive approach to electronic structure in the presence of liquid environments.

5.2 Joint density-functional theory

As shown in Chapter 2, a straightforward combination of Mermin's non-zero temperature formulation of density-functional theory[10] with Capitani *et al.*'s extensions of the zero-temperature theory to include nuclear degrees of freedom[11] leads to the following, exact variational principle for the total thermodynamic free

energy of an electron-nuclear system in a fixed external electrostatic potential $V(r)$

$$A = \min_{n_t(r),\{N_i(r)\}} \left\{ F[n_t(r), \{N_i(r)\}] + \int d^3r \; V(r) \left(\sum_i Z_i N_i(r) - n_t(r) \right) \right\}, \tag{5.1}$$

5.3 Construction of approximate functionals

Working with (2.7) requires an approximate functional $A_{lq}[\{N_i(r)\}]$ for the bulk liquid. For water this is an active area of research[12, 13, 14]. To describe water in our preliminary implementation, rather than using the functional developed in Chapter 4, for computational expediency, we developed an even simpler functional based on the ideas of Sun[12]. We first imagine minimizing over the proton density so that a single field remains, the density $N(r)$ of the oxygen nuclei, which one may view as the "molecular density" as determined by taking the oxygen nucleus to define the location of each molecule. Our version of the resulting functional then takes the form

$$\begin{aligned} &A_{lq}[N(r)] = \\ &A_{id}[N(r)] + \int N(r) \left[\epsilon_{hs}(N(r)) - aN(r) \right] d^3r \\ &-b \int N(r) \left[\int g_\sigma(r - r') N(r') \, d^3r' - N(r) \right] d^3r. \end{aligned} \tag{5.2}$$

The first term in Eq. (5.2), $A_{id}[N(r)] = k_B T \int N(r) \left(\ln \left(N(r) \lambda^3 \right) - 1 \right) d^3r$ is the analytically *exact* functional for the ideal gas, where $k_B T$ is the thermal energy and λ is the thermal de Broglie wave length of the solute molecules. In the second term, $\epsilon_{hs} \equiv k_B T \left((3/2) \left((1 - \eta)^{-2} - 1 \right) - \ln (1 - \eta) \right)$ is the Percus-Yevick approximation[15] for the free energy per particle of a system of hard spheres of diameter d over and above that of the ideal gas, where $\eta \equiv (\pi d^3/6) N(r)$ with d be-

ing the sphere diameter (fit to experimental parameters below). (In retrospect, this work should have employed the Carnahan-Starling approximation, which more accurately describes hard spheres and represents little or no computational overhead. For the range of parameters relevant here, the two approximations agree to within about 4%, and so we expect little significant change to the final results.) The constant a in this second term describes the cohesive tendency between molecules that holds the fluid together. The third term is written so that it is non-zero only if $N(r)$ is not constant, where b is a coupling constant and $g_\sigma(r) \equiv \exp(-r^2/2\sigma^2)/(2\pi\sigma^2)^{3/2}$ is a normalized Gaussian describing the range of non-local behavior.

The first two terms in Eq. (5.2) capture the properties of the bulk fluid. The two parameters a and d in these terms were adjusted to reproduce the equilibrium density and bulk modulus of water with results summarized in Table 5.1. For the final term which describes inhomogeneities, the non-local coupling strength b and the range σ were adjusted to reproduce the macroscopic surface tension of water γ and the approximate location R_b of the "bend" (as measured by the point of maximum downward curvature) of the surface tension versus sphere radius prediction of the molecular dynamics data of ten Wolde and co-workers[16]. Table 5.1 summarizes these results as well. We emphasize that although some of the parameter fits in this preliminary formulation are empirical, they do not involve any solvation free-energy data *whatsoever*.

For the coupling functional $U[N(r), n(r), V(r)]$ in (2.7), we proceed by dividing it into two parts: long-range dielectric screening $\Delta U_{sc}[n(r), V(r)]$ capturing the tendency of the molecules in the liquid to be found in orientations and polarization states that tend to screen long-range electric fields, and a short-range electron-overlap interaction $\Delta U_{el}[N(r), n(r)]$. The long-range screening depends only on

Table 5.1: Fit parameters from (5.2) with comparisons between model and experimental results (at standard conditions of 20°C and atmospheric pressure. (*) The value for $d\gamma/dR$ is theoretical[16]. (See text.)

parameters	a ($\frac{\text{J m}^3}{\text{mole}^2}$)	d (nm)	b ($\frac{\text{J m}^3}{\text{mole}^2}$)	σ (nm)
values	0.3944	0.2918	0.1561	0.4388
properties	N_b (kg/m^3)	B (GPa)	γ (mJ/m^2)	R_b (nm)
this work	998.3	2.184	71.93	3.70
experiment(*)	998.2	2.190	72.75	∼4

the electrostatics of the solute and so depends only on its electron density $n(r)$ and the nuclear electrostatic potential $V(r)$. The electron-overlap contribution depends upon contact between the solvent molecules and the solute electron density and so to some approximation depends only upon these two densities.

The lowest-order form for the electronic coupling between the liquid and the solute which is compatible with translational and rotational symmetry is then

$$\Delta U_{el}[N(r), n(r)] = \int d^3R \int d^3r \; n(r) V_{ps}(r - R) N(R).$$

Such a lowest-order coupling is a reasonable starting point as the overlap is small. With this form, the convolution kernel V_{ps} plays the role of the average potential which an electron at point r feels from a water molecule at point R, similar to the "molecular" pseudopotential of the type introduced by Cho and coworkers in the different context described above[17]. The main difference between this potential

and that of Ref. [17] is that in the present, preliminary formulation, the pseudopotential contains no information about the orientation of the molecules and so represents some sort of orientational average. To optimize numerical convergence, we choose to fit $V_{ps}(r)$ to the sum of two origin-centered Gaussians of adjustable width and amplitude for a total of four adjustable parameters,

$$V_{ps}(r) = A_1 e^{-\frac{r^2}{2\sigma_1^2}} + A_2 e^{-\frac{r^2}{2\sigma_2^2}}.$$

We then adjusted these parameters to reproduce the orientationally averaged interaction of a water molecule with an atom of neon as a function of distance. Figure 5.1 summarizes the results. The parameters that we found are

$$A_1 = 0.0765; \sigma_1 = 2.045; A_2 = -0.065; \sigma_2 = 2.165.$$

With this simple form, we were able to reproduce the average interaction to within 1 millihartree ($\sim$ 0.63 kcal/mole) for all distances beyond 2Å. (Smaller distances are not very relevant as the interaction becomes very repulsive. For comparison, at room temperature, $k_B T = 0.93$ mH.) Here, there is no fitting to empirical data, and the pseudopotential is truly *ab initio*.

Next, the screening term depends upon the long-range electrostatic potential of the solute and the tendency of the solvent molecules to orient and polarize along the resulting fields. Here, we go a small step beyond our screening model in Chapter 3, and model the screening as the electrostatic response in the presence of a linear, scalar (i.e., non-tensor), but now *non-local* dielectric function. Note that although this is a small improvement to the description of the long wavelength interactions, the overall model which we introduce here is much more sophisticated than that of Chapter 3 in that it includes an explicit description of the solvent in terms of a density functional (thus accounting cavitation effects) and also includes a short-

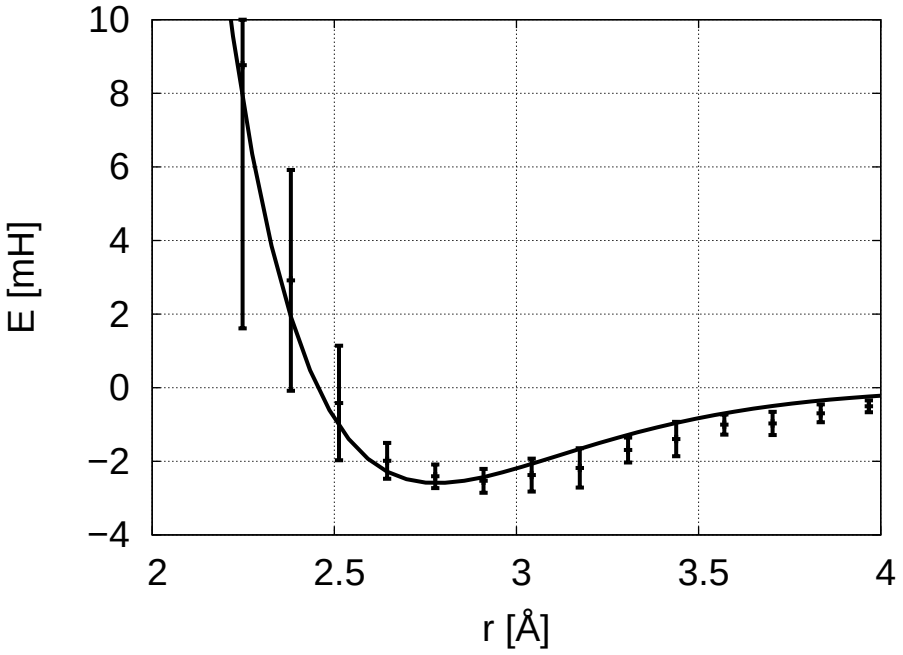

Figure 5.1: Comparison of energy of interaction of water molecule with an atom of neon as a function of neon-oxygen distance: results from orientation independent pseudopotential (solid curve), orientally averaged *ab initio* data (centers of error bars), typical (1σ) range of values as a function of orientation (range of error bars).

range contact interaction (thus accounting repulsion and dispersion effects). The particular model we have explored for the dielectric function is

$$\epsilon(r, r') \equiv \delta(r - r') + \frac{4\pi\chi_b}{N_b^2} N(r) f(r - r') N(r'),$$

where $\delta(r)$ is the Dirac-delta function, $f(r)$ is a short-ranged function integrating to one, and N_b and χ_b are the density and static dielectric polarizabilities, respectively, of the bulk liquid. This choice ensures a smooth transition from the dielectric constant of the bulk to that of vacuum over the length-scale of $f(r)$. The choice to include both $N(r)$ and $N(r')$ is motivated both by the need for $\epsilon(r, r')$ to be symmetric and by the notion that the response at point r to a field at point r' depends on the density of molecules at both locations. The connecting function $f(r)$ was chosen to be a Gaussian of width σ=2.25 bohr=$\sim$1.190 Å, somewhat larger than the O-H bond distance in water. The motivation for using this value of σ is that, at lower values, dielectric screening at short length-scales is so effective that the system may lower its energy by bringing fluid density $N(r)$ into the atomic cores and the system thus becomes numerically unstable. We stress, however, that once stability was achieved, the final results were not sensitive to the choice of this parameter (typically 10% variation in the solvation energy over the range $\sigma = 1.5$ bohr to $\sigma = 2.5$ bohr) and that this parameter was in no way adjusted to reproduce experimental solvation energies. In the future, a direct description of the electric polarization in terms of the orientational state of the solvent would capture dielectric effects directly and remove the need for constructing such a simple model.

Finally, in conjunction with a nonlocal dielectric response, a term must be added to the energy functional to help prevent the aforementioned numerical issues associated with penetration of the solvent density into the cores of the atoms. To avoid this, we added a short-ranged repulsive potential of the form

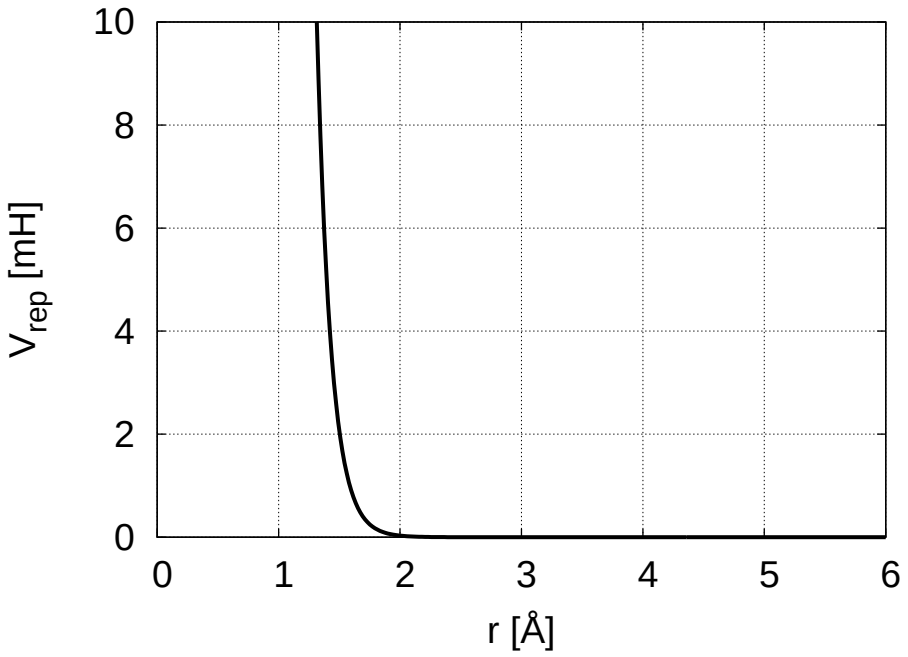

Figure 5.2: Short-ranged repulsive potential added to prevent collapse of liquid density $N(r)$ into the strong electric fields within the atomic cores. Once prevention of this artificial collapse is achieved, the final results are insensitive to the choice of this potential.

$\int V_{rep}(r)N(r)\,d^3r$ inside the atomic cores to prevent the overlap of the solvent with the nuclei, where $V_{rep}(r)$ is taken to be a rapidly decaying exponential function (rounded within $\sim$0.25 Å of the origin) of constant 8.44 Å^{-1}, leading to an apparent hard wall at thermal energy scales near 1.5 Å(Figure 5.2). Again, once the system is numerically stable, the results are not sensitive to the form of the repulsion (typically 1% changes in solvation energy) so long as the repulsion effectively cuts off before the natural point of closest approach of the solvent at $\sim$2 Å. (See Figure 5.3 and the corresponding discussion below.)

5.4 Results and conclusions

The meaningful physical quantities predicted by joint-density functional theory include not only the free energy A but also the liquid density $N(r)$. Under certain circumstances, the later is accessible directly in experiments. For instance, when studying the solvation of a water molecule with liquid water, the density $N(r)$ in our formulation gives the density of oxygen nuclei given a fixed location for one water molecule. As observed by Percus [18], the spherical average of $N(r)$ thus corresponds to the oxygen-oxygen pair distribution function $g_{OO}(r)$ measured in experiments. Figure 5.3 shows our results for this quantity. In good agreement with both x-ray and neutron scattering experiments[19], we find $N(r)$ to be essentially zero until a radius of $\sim$2.0 Å, at which point the density rises rapidly, overshooting the bulk density before finally approaching it. The experiments do show a much more pronounced peak and much more structure in the form of oscillations which occur beyond 2.5 Å. We believe that these discrepancies are due to the over simplified model we are using for $A_{lq}[N(r)]$ in (5.2) and that a better liquid density-functional would improve this. Generally, the coordination number for a liquid is defined as the integral of g_{OO} from $r = 0$ to the location of the first minimum after the coordination peak. In our case there are no such oscillations. However, if we define the coordination number as the integral of g_{OO} up to 3.6 Å, the last point before the bulk value of unity is obtained, we find a coordination of 5.3, relatively close to the value of approximately four measured in liquid water and far from the close packed value near twelve typically found in simple fluids. Thus, our model, as simple as it is, captures enough of the physics of water to reflect the hydrogen bonding network which leads to tetrahedral coordination. The model also appears to reflect the correct energetics and to give a correct *ab ini-*

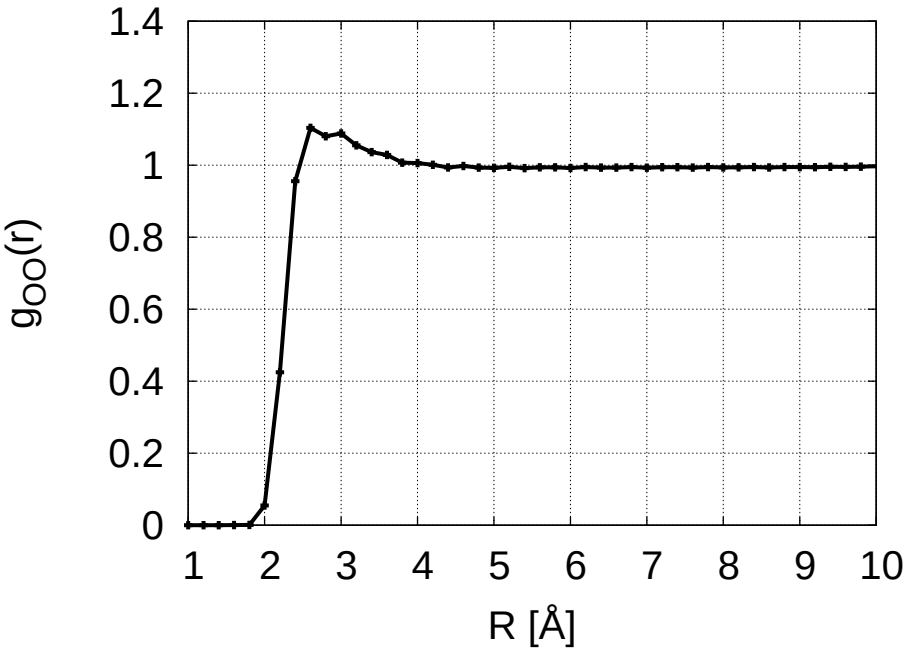

Figure 5.3: Spherical average of $N(r)$ about the oxygen nucleus of an explicit water molecule in solution scaled to the bulk liquid density, corresponding to the correlation function $g_{OO}(r)$ measured in experiments on liquid water.

tio prediction of the boundary position of the cavity outside of which the fluid is excluded. To our knowledge, this is the first accurate determination of such a boundary directly from first principles. As solvation energies are known to be quite sensitive to the construction of the boundary, this success gives a strong advantage to the current approach.

Finally, Figure 5.4 summarizes the comparison of the free energies predicted by the implementation described above with both experiment and the predictions of state-of-the-art continuum solvation models. Our joint density-functional theory results are clearly superior to dielectric-cavity-only calculations and are arguably better than state-of-the-art continuum methods that include cavity corrections. It is particularly satisfying to see that, without any fitting or *ad hoc* adjustments,

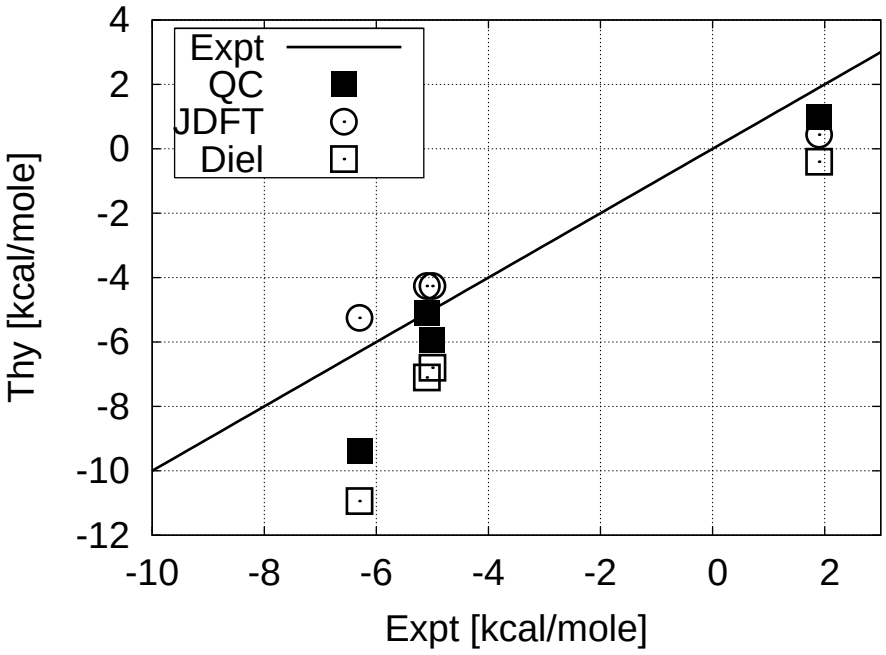

Figure 5.4: Computed (vertical axis) versus experimental (horizontal axis) solvation energies for water, ethanol, methanol and methane (from left to right): perfect agreement (diagonal line), published quantum chemistry values ([20] for all but water, [21] for water) with dielectric contribution only (open squares) and including cavitation terms (closed squares), preliminary results from joint density functional theory (open circles).

the hydrophobicity of methane is predicted correctly. We emphasize, however, that this agreement does not imply that we have correctly captured all of the underlying physics. More direct, microscopic physics should be built into the functionals, particularly in the description of dielectric screening effects. We feel that the quality of the current results, *without adjustment of parameters*, suggests that incorporation of more microscopic physics into the design of the functionals has the potential to lead to yet more reliable results in the future.

Although the results of this preliminary implementation are already superior

in that they involve no fitting to solvation energies and are of comparable quality to the state-of-the-art, there are a number of weaknesses in the preliminary implementation, namely (1) the lack of orientational dependence in the pseudopotential, (2) an artificial separation of the dielectric response from the internal orientational correlations of the liquid, (3) an over simplified, linear description of the dielectric response with an *ad hoc* nonlocal length scale, (4) the resulting need to artificially prevent the solvent from overlapping the nuclei. Most of these weaknesses can be addressed by a formulation informed of orientational ordering by including knowledge of the underlying hydrogen bonding network of water. This would allow for the use of orientation-dependent pseudopotentials and would naturally capture nonlocal and nonlinear effects in the dielectric response.

Bibliography

[1] M. Payne *et al.*, Rev. Mod. Phys. **64**, 1045 (1992).

[2] J. Seminario, *Recent Developments and Applications of Modern Density Functional Theory* (Elsevier, Amsterdam, 1996).

[3] J. Tomasi and M. Persico, Chem. Rev. **94**, 2027 (1994).

[4] J. Tomasi, B. Menucci, R. Cammi, and M. Cossi, in *Theoretical Aspects of Biochemical Reactivity*, edited by G. Naray-Szabo and A. Warshel (Kluwer, Dordrecht, 1997), p. 1.

[5] J.-L. Rivail and D. Rinaldi, in *Computational Chemistry, Review of Current Trends*, edited by J. Leszczynski (World Scientific, New York, 1995), p. 139.

[6] C. J. Cramer and D. G. Truhlar, Chem. Rev. **99**, 2161 (1999).

[7] F. J. Luque *et al.*, Phys. Chem. Chem. Phys. **5**, 3827 (2003).

[8] J. Dzubiella, J. M. J. Swanson, and J. A. McCammon, Phys. Rev. Lett. **96**, 087802 (2006).

[9] M. Young, B. Jayaram, and D. Beveridge, J. Phys. Chem. B **102**, 7666 (1998).

[10] N. D. Mermin, Phys. Rev. **137**, A1441 (1965).

[11] J. Capitani, R. Nalewajski, and R. Parr, J. Chem. Phys. **76**, 568 (1982).

[12] S. X. Sun, Phys. Rev. E **64**, 021512 (2001).

[13] T. F. Meister and D. M. Kroll, Phys. Rev. A **31**, 4055 (1985).

[14] R. Ramirez and D. Borgis, J. Phys. Chem. **109**, 6754 (2005).

[15] J. K. Percus and G. J. Yevick, Phys. Rev. **110**, 1 (1957).

[16] P. R. ten Wolde, S. X. Sun, and D. Chandler, Phys. Rev. A **137**, 1441 (1965).

[17] K. S. Kim *et al.*, Phys. Rev. Lett. **76**, 956 (1996).

[18] J. K. Percus, Phys. Rev. Lett. **8**, 462 (1962).

[19] G. Hura, J. M. Sorenson, R. M. Glaeser, and T. Head-Gordon, Journal of Chemical Physics **113**, 9140 (2000).

[20] B. Marten *et al.*, J. Phys. Chem. **100**, 11775 (1996).

[21] T. Truong and E. Stefanovich, Chem. Phys. Lett. **240**, 253 (1995).